CPT1A Mediates Radiation Sensitivity in Colorectal Cancer

Running title: Radiation sensitivity in CRC via CPT1A

Zhenhui Chen[1, #], Lu Yu[2, #], Zhihao Zheng[2, #], Xusheng Wang[2], Qiqing Guo[2], Yuchuan Chen[3], Yaowei Zhang[2], Yuqin Zhang[2], Jianbiao Xiao[4], Keli Chen[5], Hongying Fan[1, *], Yi Ding[2, *]

[1]Department of Microbiology, Guangdong Provincial Key Laboratory of Tropical, Disease Research, School of Public Health, Southern Medical University, Guangzhou, China

[2]Department of Radiation oncology, Nanfang Hospital, Southern Medical University, Guangzhou, China

[3]State Key Laboratory of Organ Failure Research, Key Laboratory of Infectious Diseases Research in South China, Ministry of Education, Guangdong Provincial Key Laboratory of Viral Hepatitis Research, Guangdong Provincial Clinical Research Center for Viral Hepatitis, Department of Infectious Diseases, Nanfang Hospital, Southern Medical University, Guangzhou, China

[4]Department of Pathology, Nanfang Hospital and School of Basic Medical Science, Southern Medical University

[5]HuiQiao Medical Center, Nanfang Hospital, Southern Medical University, Guangzhou, China

[*] **Correspondence Author:**

Yi Ding E-mail: dy512@smu.edu.cn

Hongying Fan E-mail: gzfhy@smu.edu.cn

[#]**These authors have contributed equally to this work.**

Abstract

The prevalence and mortality rates of colorectal cancer (CRC) are increasing worldwide. Radiation resistance hinders radiotherapy, a standard treatment for advanced CRC, leading to local recurrence and metastasis. Elucidating the molecular mechanisms underlying radioresistance in CRC is critical to enhance therapeutic efficacy and patient outcomes. Bioinformatic analysis and tumour tissue examination were conducted to investigate the CPT1A mRNA and protein levels in CRC and their correlation with radiotherapy efficacy. Furthermore, lentiviral overexpression and CRISPR/Cas9 lentiviral vectors, along with *in vitro* and *in vivo* radiation experiments, were used to explore the effect of CPT1A on radiosensitivity. Additionally, transcriptomic sequencing, molecular biology experiments, and bioinformatic analyses were employed to elucidate the molecular mechanisms by which CPT1A regulates radiosensitivity. CPT1A was significantly downregulated in CRC and negatively correlated with responsiveness to neoadjuvant radiotherapy. Functional studies suggested that CPT1A mediates radiosensitivity, influencing reactive oxygen species (ROS) scavenging and DNA damage response. Transcriptomic and molecular analyses highlighted the involvement of the peroxisomal pathway. Mechanistic exploration revealed that CPT1A downregulates the FOXM1-SOD1/SOD2/CAT axis, moderating cellular ROS levels after irradiation and enhancing radiosensitivity. CPT1A downregulation contributes to radioresistance in CRC by augmenting the FOXM1-mediated antioxidant response. Thus, CPT1A is a potential biomarker of radiosensitivity and a novel target for overcoming radioresistance, offering a future direction to enhance CRC radiotherapy.

Keywords: Colorectal cancer, CPT1A, reactive oxygen species, radiosensitivity, FOXM1

Introduction

Colorectal cancer (CRC) is the second-highest cause of cancer-related mortality(Siegel, Wagle, Cercek, Smith, & Jemal, 2023). Radiotherapy is crucial for CRC management, especially in patients with locally advanced rectal cancer ($cT_{3-4}N_{+}$)(Glynne-Jones et al., 2017). Neoadjuvant therapies show clinical or pathological complete response in 16–30% of patients, realising downstaging in approximately 60% of patients, significantly enhancing local control, and facilitating curative surgery(Cercek et al., 2018). Moreover, radiotherapy is beneficial in initially unresectable and recurrent cases with limited metastasis to organs, such as the liver and lungs(Cervantes et al., 2023). Nonetheless, the effectiveness of radiotherapy is affected by radioresistance, which precipitates tumour relapse and metastasis and currently lacks an efficacious clinical resolution. Unlocking the molecular mechanisms underlying CRC radioresistance will enhance outcomes and improve patient prognoses.

Reactive oxygen species (ROS) are byproducts of normal cellular metabolism occurring in organelles, such as mitochondria, endoplasmic reticulum, and peroxisomes(Bhattacharyya, Chattopadhyay, Mitra, & Crowe, 2014). Within mitochondria, 90% of cellular ROS are generated by complexes I, II, and IV of the electron transport chain(Glasauer & Chandel, 2014). Exogenous stimuli, including radiation, can cause significant, acute elevations in ROS levels(Hecht, Zocchi, Alimohammadi, & Harris, 2024). ROS function ambivalently in the intracellular signalling and redox homoeostasis of tumour cells(Shah, Ibis, Kashyap, & Boussiotis, 2023). ROS amplify oncogenic phenotypes, such as proliferation and differentiation, hasten the accumulation of metastasis-inducing mutations, and aid tumour cell survival under hypoxic conditions(Palma et al., 2023). However, excess ROS precipitate apoptosis and other cell death types from oxidative stress(Palma et al., 2023). Thus, intracellular ROS generation is meticulously monitored and regulated by a comprehensive ROS-scavenging system encompassing antioxidants and antioxidative enzymes(Palma et al., 2023; Shah et al., 2023).

Radiation ionises water molecules, creating an intracellular surge of ROS, which

indirectly cause two thirds of DNA damage(Chio & Tuveson, 2017). Consequently, ROS scavenging inevitably influences cancer cell radiosensitivity(Skvortsova, Debbage, Kumar, & Skvortsov, 2015). Increased expression and activity of antioxidative enzymes, such as peroxidase (POD), catalase (CAT), glutathione peroxidase, and glutathione reductase, are correlated with radiosensitivity(Hecht et al., 2024).

Carnitine palmitoyltransferase 1 (CPT1) is an outer mitochondrial membrane that catalyses the rate-limiting step of fatty acid oxidation and is absent in several tumours(Melone et al., 2018). The CPT1 family contains three isoforms: CPT1A, CPT1B, and CPT1C. Research on CPT1A has been detailed(Schlaepfer & Joshi, 2020). CPT1A is critical to cancer cell growth, survival, and drug resistance, making it an attractive target(Qu, Zeng, Liu, Wang, & Deng, 2016). CPT1A also interacts with other key pathways and factors regulating gene expression and apoptosis in cancer cell(Qu et al., 2016). However, its role in CRC and radiotherapy resistance is unclear.

Forkhead box M1 (FOXM1) is a critical transcription factor for many cellular processes(Kalathil, John, & Nair, 2020). Besides benefitting normal cell functions, it also regulates cancer processes, including growth, metastasis, and recurrence(Alimardan et al., 2023; Khan, Khan, Ahmad, Fatima, & Nasser, 2023). FOXM1 also affects radiotherapy outcomes in many cancer types, including colorectal cancer(Kwon et al., 2021; Li et al., 2022; N. Liu et al., 2019; Pal et al., 2018; Takeshita et al., 2023; Xiu, Sui, Wang, & Zhang, 2018).

Previously, we found that various metabolic pathways, including fatty acid metabolism, are closely related to tumour radioresistance. Therefore, this study mainly focused on CPT1A, which affects CRC radiosensitivity, to reveal novel therapeutic strategies to mitigate radiotherapy resistance and improve clinical outcomes.

Methods

Reagents and materials

The reagent suppliers are indicated in Supplementary Table 1.

Bioinformatic analyses

Raw mRNA expression profiles and clinical features from GSE9348, GSE20916, GSE37364, GSE44076, GSE68468, and GSE110223 were downloaded from GEO (http://www.ncbi.nlm.nih.gov/geo/). The *CPT1A* mRNA expression in cancer and paired normal tissues was analysed using ualcan (ualcan.path.uab.edu/) (Chandrashekar et al., 2022). Correlation analyses between genes were conducted using GEPIA2 (http://gepia2.cancer-pku.cn/) (Tang, Kang, Li, Chen, & Zhang, 2019). Transcription factor prediction and promoter binding site analysis for SOD1, SOD2, and CAT were conducted using the hTF target database (http://bioinfo.life.hust.edu.cn/hTFtarget#) (Q. Zhang et al., 2020). Additionally, JASPAR (http://jaspar.genereg.net/) was used to predict the binding sites of FOXM1(Rauluseviciute et al., 2024).

RNA isolation and qRT-PCR

All rectal adenocarcinoma and paired normal tissues used for RNA isolation and qRT-PCR were provided by the Department of Pathology, Nanfang Hospital of Southern Medical University (n=48). Specimen collection was approved by the Ethics Committee of the Nanfang Hospital, Southern Medical University. Total RNA was extracted using TRIzol following the manufacturer's instructions. cDNA was generated using the Evo M-MLV RT Mix Kit. mRNA expression was analysed using the SYBR Green Premix Pro Taq HS qPCR Kit on a QuantStudio6 Real-time PCR system, and β-actin was used for normalisation. Data were analysed using the $2^{-\Delta\Delta CT}$ method. The PCR primers are listed in Supplementary Table 2.

Protein extraction and western blotting

Rectal adenocarcinoma and paired normal tissues for western blotting were from our Department of Pathology (n=32). Proteins were extracted from tissues and cells using a protein extraction kit, according to the manufacturer's instructions. Briefly, Nanodrop was used to determine the protein concentration. The proteins were mixed in a 4:1 ratio with 5×loading buffer and denatured at 100 °C in a water bath for 5 min. Subsequently, 20 μg of proteins were subjected to SDS-PAGE at 95 V. Subsequently, proteins were

147 transferred onto PVDF membranes at a constant current. The membrane was blocked
148 with 5% BSA and incubated with the corresponding primary antibody overnight at 4 °C.
149 Subsequently, the membrane was incubated with an HRP-conjugated secondary
150 antibody (1:2000 dilution), and protein levels were detected using enhanced
151 chemiluminescence.

152 **Immunohistochemistry**

153 All colon cancer (n=76) and rectal adenocarcinoma tissues (n=45) were collected
154 before treatment and sectioned at 4 μm. Clinicopathological features of the patients
155 were provided by the Department of Pathology (Table 1). Staining intensity was
156 independently evaluated by two senior pathologists.

157 **Cell culture and lentiviral infection**

158 The CRC cell lines HCT-15, RKO, HCT 116, HT-29, Caco-2, SW480, and SW620 were
159 purchased from ATCC (Manassas, VA, USA). All cell lines were cultured in RPMI-
160 1640 medium supplemented with 10% FBS. Cells were cultured at 37 °C with 5% CO_2.
161 To establish radiation-resistant strains, HCT-15-25F and HCT-15-5F cells were
162 generated using both conventional fractionated irradiation (2 Gy/fraction, 25 fractions,
163 5 fractions/week over 5 weeks) and large-fractionated irradiation (5 Gy/fraction, 5
164 fractions, for 1 week).

165 The full-length lentiviral expression of *CPT1A* with puromycin was constructed by
166 VectorBuilder. *CPT1A*-targeting CRISPR/Cas9 lentiviral vectors (hCpt1a[gRNA#1]:
167 AAATCTCTAC**TACACGGCCGATGTTACGAC**AGGTACCGTCCTT,
168 hCpt1a[gRNA#2]:
169 AGAAGGTAAG**GACGGTACCTGTCGTAACAT**CGGCCGTGTAGTA,
170 hCpt1a[gRNA#3]:
171 CTGAACACTC**CTGGGCAGATGCGCCGATCG**TGGCCCACCTTTG) with RFP
172 and Puro were constructed by VectorBuilder. Infection and *in vitro* transfection of cell
173 lines were performed following the manufacturer's protocol. The lentiviral full-length
174 expression of *FOXM1* with G418 was constructed using VectorBuilder.

175 **Colony formation assay and multi-target single-hit survival model**

176 The radiosensitivity of all human CRC cell lines was determined using a colony

formation assay (CFA) with a multi-target single-hit model to the surviving fractions. Cells were plated in 6-well plates and irradiated at doses of 0, 2, 4, 6, 8, and 10 Gy (6 MeV X-rays). The cells were then cultured for 10 d, stained with 1% crystal violet, and quantified using ImageJ version 1.8.0. The surviving fraction for each dose was calculated using the following formula:

[(number of surviving colonies at dose X) / (number of cells seeded at dose X (average colonies arising from non-irradiated cells (0 Gy)) / number of non-irradiated cells seeded)]. Survival curves were used to develop the multi-target single-hit model, $SF = 1 - (1 - e^{-D/D0}) \times N$, where SF is the surviving fraction, D is the radiation dose, and N is the extrapolation number.

Comet assay

The comet assay was performed as previously described(Yu et al., 2022). Briefly, slides were covered with 100 μL of pre-warmed normal melting point agarose (2%) and placed on ice to solidify the first gel layer. Cells irradiated with 6 Gy were digested to obtain a cell suspension. Ten microliters of the cell suspension were mixed with 80 μL of pre-warmed low melting point agarose (0.75%) and poured onto the slides. The slides were dipped in a cold lysis solution for 2 h. After cell lysis, the slides were placed in a horizontal electrophoresis chamber filled with cold TAE solution, incubated for 25 min in the dark, and electrophoresed (1 V/cm). The slides were then neutralised in PBS for 5 min and stained with propidium iodide (PI) or DAPI. Comet images were captured using a fluorescence microscope. The percentage of DNA in the tail was analysed using the CASP 1.2.3 beta 1.

Animal model

All animal experiments were approved by the Institutional Animal Care and Use Committee of Nanfang Hospital. Male BALB/c nude mice (5 weeks old) were purchased from the Southern Medical University Laboratory Animal Center, China and raised under specific pathogen-free conditions. All *in vivo* experiments were performed following institutional guidelines. To develop the xenograft tumour model, 5×10^6 cells were subcutaneously injected into the left flank of mice. On reaching a volume of 100 mm^3, the tumours were irradiated twice at 8 Gy, and other parts of the mouse body

were protected with a lead shield. The tumour volume was measured using Vernier callipers and calculated as 1/2 × length × width × width. After the mice were euthanised with phenobarbital sodium, the tumours were excised, weighed, and embedded in paraffin for further experiments.

Transcriptomics

HCT 116-NC and HCT 116-KO cells were collected and sent to RIBOBIO (Guangzhou, China) for polyA-seq transcriptome sequencing. RNA extraction, library preparation, and sequencing were performed according to the manufacturer's instructions. To identify the differentially expressed genes (DEGs) between the two groups, the expression level of each transcript was calculated according to the transcript per million reads method. RSEM was used to quantify the gene abundance. Differential expression analysis was performed using DESeq2(S. Liu et al., 2021). Genes with $|\log_2(\text{fold change})|>1$ and $P<0.05$ were considered significantly differentially expressed. In addition, functional enrichment analysis, including using Gene Ontology (GO) and Kyoto Encyclopedia of Genes and Genomes (KEGG), was performed to identify significantly enriched DEGs in GO terms and metabolic pathways at a Bonferroni-corrected P-value of 0.05 compared with the whole-transcriptome background. The heatmap and volcano of mRNA sequencing were conducted on ImageGP (www.bic.ac.cn/ImageGP) (Tong Chen, 2022). GO functional enrichment and KEGG pathway analyses were performed using the ClusterProfiler package in R(Wu et al., 2021).

ROS detection

ROS were stained with a 2,7-dichlorodihydrofluorescein diacetate (DCFH-DA) probe and detected using flow cytometry. Briefly, the probe was diluted in cell culture media at a 1:1000 ratio to yield a final concentration of 10 μmol/L. The culture medium was replaced with 1 mL of DCFH-DA solution. The cells were incubated at 37 °C for 20 min. After incubation, the cells were washed thrice with serum-free medium to remove any excess DCFH-DA.

One hour after 6 Gy irradiation, the cells were digested into single-cell suspensions and washed once with PBS. Finally, cells were resuspended in PBS, and the

fluorescence intensity was analysed using flow cytometry at excitation and emission wavelengths of 488 and 525 nm, respectively.

GSH/oxidised GSH ratio

Cells (5×10^5 cells/well) were seeded into 10 cm wells until they reached 80% confluence. One hour after 6 Gy irradiation, the GSH/oxidised GSH (GSSG) ratio was determined using a GSH/GSSG ratio detection assay kit following the manufacturer's protocols.

Enzyme activity

Cells (5×10^5 cells/well) were seeded into 10 cm wells until reaching 80% confluence before. One hour after irradiation with 6 Gy, crude enzyme extract was prepared. The cells were digested, collected, and centrifuged to remove the supernatant. Next, 1 mL of HPLC-grade water was added to each pellet. The cells were disrupted by ultrasonication (20% power, 3 s on and 10 s off, repeated 25–40 times). The resulting mixture was centrifuged at 8000 ×*g* and 4 °C for 10 min, and the supernatant was collected as the crude enzyme extract. The enzyme activities of SOD1, SOD2, CAT, and POD were detected using respective enzyme activity kits, according to the manufacturer's protocols.

Statistical analysis

Data are expressed as the mean ± standard deviation (SD), and P-values <0.05 were considered statistically significant in all experiments. Data were analysed using one-way analysis of variance (ANOVA), Spearman's correlation, and Kaplan–Meier estimates. Statistical analyses were performed using SPSS software (version 20.0). All experiments were performed in triplicate.

Results

Low expression of CPT1A in CRC tumours

Analysis of CRC mRNA sequencing arrays from GEO consistently indicated low *CPT1A* mRNA levels in CRC (Figure 1A). The transcript levels of *CPT1A* were lower

in most colon cancers (19/24 pairs) than in the adjacent non-tumour tissues (Figure 1B). Meanwhile, CPT1A protein levels were lower in most CRC tissues (14/16 pairs) than in the adjacent non-tumour tissues (Figure 1C). Further exploration of CPT1A expression in TCGA revealed that CPT1A mRNA levels were significantly lower in colon adenocarcinoma (COAD) tissues than in the adjacent non-tumour tissues (Figure 1D). Similar results were observed for rectal adenocarcinoma (READ) (Figure 1E). Immunohistochemistry (IHC) staining of the cancer-adjacent borders of two patients showed that CPT1A protein levels were lower in CRC tissues than in the nearby non-tumour tissues (Figure 1F). These findings provide comprehensive evidence supporting the downregulation of *CPT1A* expression at both mRNA and protein levels in CRC.

Low-CPT1A CRC exhibits radioresistance and poor overall survival

Based on the IHC scores, patients were divided into CPT1A high- and low-expression groups (Figure 2A). Kaplan–Meier survival analysis indicated that low CPT1A-expressing patients had low overall survival (OS) (Figure 2B). Survival analysis of READ patients with low CPT1A using GEPIA also suggested a low OS; the difference was statistically close but not significant (P=0.061, Figure 2C). To further investigate the correlation between CPT1A and radiotherapy efficacy, IHC staining and scoring for CPT1A were performed on samples from 43 patients with rectal cancer who received neoadjuvant radiochemotherapy. Among patients with a tumour regression grade (TRG) score of 1, which indicates a minimal number of residual tumour cells, a high IHC score for CPT1A is often observed. Conversely, patients with a TRG score of 2, indicating more residual tumour cells, exhibited relatively lower IHC staining intensity and overall scores (Figure 2D). A comparison of groups with TRG 2–3 and TRG 1 revealed significantly higher IHC scores in the TRG 1 group (Figure 2E). The TRG and IHC scores for CPT1A showed a negative correlation (R=-0.3430 and P=0.024) (Figure 2F). In summary, low CPT1A

expression was associated with poor OS, high TRG scores, and a high probability of radioresistance.

Decreased CPT1A expression contributes to radiation resistance in CRC cells

Through a CFA and multi-target single-hit survival model, we found that SW480, Caco-2, SW620, HT-29 and cells were more resistant to radiation than HCT15, RKO, and HCT 116 cells (Supplementary Figure 1A, B, Supplementary Table 3). Furthermore, the background expression levels of CPT1A in the above cells revealed that CPT1A transcription and protein levels were higher in radiation-resistant cells than in radiosensitive cells (Supplementary Figure 1C, D).

Accordingly, we constructed stable CRC cell lines with CPT1A knockout/overexpression. We transfected the CRISPR/Cas9 lentivirus into HCT 116 cells (highest CPT1A expression and radiosensitive) and used western blotting to verify that the knockout efficiency of the 2nd site was the highest, while mRNA levels were significantly reduced (Figure 3A, B). We used the 2nd knockout site for subsequent *in vitro* and *in vivo* experiments. We also transfected the CPT1A-overexpressing lentivirus into SW480 cells (lowest CPT1A expression and radioresistant) and verified that CPT1A protein and mRNA levels increased (Figure 3A, B).

The CFA and multi-target single-hit survival model suggested that radioresistance increased with *CPT1A* knockout (D0=1.526 vs. 1.993, $P<0.05$, Figure 3C, D), whereas the radioresistance of cells decreased with *CPT1A* overexpression (D0=2.724 vs.1.963, $P<0.01$, Figure 3E, F). The comet assay suggested that the proportion of DNA in the tail of cells decreased with CPT1A knockout, indicating improved damage repair. With *CPT1A* overexpression, the proportion of DNA in the tail increased, indicating reduced damage repair capabilities (Figure 3G). We also detected γ-H2A.X expression at different time points after 6 Gy irradiation; with *CPT1A* knockout, γ-H2A.X disappeared from cells faster, indicating improved cell

damage repair (Figure 3H). With CPT1A overexpression, the disappearance rate of γ-H2A.X in cells was slower, remaining detectable even after 24 hours, indicating diminished cellular repair capability (Figure 3I). Collectively, our data suggest that CPT1A radiosensitizes intrinsically radioresistant cells.

We generated radioresistant cell lines (HCT-15-25F and HCT-15-5F) from the HCT-15 parent line by fractionated irradiation (Supplementary Figure 2A). Using CFAs and the multi-target single-hit survival model, we observed increased radioresistance in these new cell lines, as indicated by higher D0 values than those of the parental cells (HCT-15 D0=2.957, HCT-15-5F D0=3.240, HCT-15-25F D0=3.822) (Supplementary Figures 2B, C). We also found significantly decreased CPT1A protein expression in HCT-15-25F and HCT-15-5F cells compared with that in the original cells (Supplementary Figure 2D). Thus, HCT-15-25F cells were selected for further analysis. Transfection with the *CPT1A*-overexpressing lentivirus led to stable overexpression in HCT-15-25F cells (Supplementary Figure 2E). To assess the impact of CPT1A overexpression on DNA repair capacity, we monitored γ-H2A.X expression at different time points following 6 Gy irradiation. *CPT1A* overexpression resulted in a slow disappearance of intracellular γ-H2A.X, suggesting enhanced DNA damage repair capability (Supplementary Figure 2F). CFAs and the multitarget single-hit survival model revealed that *CPT1A* overexpression increased the radiosensitivity of radioresistant cells (D0=2.871 vs. 2.581, $P<0.05$; Supplementary Figures 2G, H), indicating that CPT1A exerts a radiosensitizing effect in inducible radioresistant cell lines.

Diminished CPT1A expression *in vivo* also leads to tumour radioresistance

To further validate the impact of CPT1A on radiation resistance *in vivo*, we established a xenograft model using HCT116-NC and HCT116-KO cell lines in nude mice (Figure 4A). *CPT1A*-stabilising knockout increased tumour weights in mice, which persisted after radiotherapy (Figure 4B), suggesting that *CPT1A* knockout promotes tumour growth and confers increased resistance to radiation. IHC staining

demonstrated a significant increase in Ki-67 staining intensity and the percentage of positive cells in *CPT1A* knockout tumours, indicating enhanced proliferative capacity that was further pronounced after radiotherapy (Figure 4C, D). Similarly, we performed xenograft model experiments using the SW480-RFP and SW480-OE cell lines (Figure 4E). CPT1A overexpression resulted in reduced tumour weight in mice, a trend that persisted even after radiotherapy (Figure 4F). These findings suggested that CPT1A overexpression inhibits tumour growth and sensitizes tumour cells to radiation. IHC staining for Ki-67 revealed significantly decreased staining intensity and percentage of positive cells in CPT1A-overexpressing tumours, indicating weakened proliferative capacity, which was further accentuated after radiotherapy (Figure 4G, H).

Low CPT1A levels accelerate post-radiation ROS scavenging

The gene expression heatmap showed high consistency among replicates for both HCT 116-NC and HCT 116-KO cells (Supplementary Figure 3A). With *CPT1A* knockdown, we found 363 upregulated and 1290 downregulated genes ($|\log_2(\text{fold change})|>1$ and $P<0.05$) (Supplementary Figure 3B). We conducted KEGG pathway analysis and GO annotation for all DEGs (Figure 5A; Supplementary Figure 3 C-E), showing that the main enriched pathways were in peroxisomes, cell cycle nucleotide excision repair, and fatty acid degradation (Figure 5A). Peroxisomes are important organelles that maintain cellular redox balance by clearing ROS. Therefore, we targeted peroxisomal pathways. ROS levels in the cells were dynamically balanced, including ROS production and scavenging (Figure 5B). To investigate the effect of CPT1A on ROS, we examined them in stable *CPT1A* knockout/overexpression cells following 6 Gy irradiation and 1 h of incubation with DCFH-DA (Figure 5C). The total ROS levels in *CPT1A* knockout cells decreased, whereas those in *CPT1A*-overexpressing cells increased (Figure 5D). The main mechanism by which cells produce ROS under irradiation is through the X-ray ionisation of water molecules, which far exceeds those from oxidative phosphorylation and NOX enzymes (Figure

5B). Therefore, we speculated that the regulation of CPT1A by intracellular ROS levels may be attributed to increased ROS scavenging. We examined the GSH/GSSG ratio (Figure 5E, F) and SOD (Figure 5G, H), CAT (Figure 5I), and POD enzyme activities (results were unchanged, data not shown) in stable *CPT1A* knockout/overexpression cells; in *CPT1A* knockout cells, the GSH/GSSG ratio and SOD and CAT enzyme activities increased, and these changes were also observed under 6 Gy irradiation (Figure 5I). In contrast, in *CPT1A*-overexpressing cells, the GSH/GSSG ratio and SOD and CAT activities decreased, and these changes were also observed after 6 Gy irradiation (Figure 5I).

We further validated the effect of CPT1A on ROS scavenging in radioresistant cells. Total ROS significantly reduced in radioresistant cells compared to those in HCT-15 control cells following 6 Gy irradiation (Supplementary Figure 4A, C). Furthermore, *CPT1A* overexpression increased total ROS levels in radioresistant cells (Supplementary Figure 4B, D), suggesting that CPT1A enhances ROS accumulation in radioresistant cells. Additionally, we assessed the GSH/GSSG ratio (Supplementary Figure 4E, F) and SOD (Supplementary Figure 4G, H), POD (Supplementary Figure 4I, J), and CAT enzyme activities (Supplementary Figure 4K) in radioresistant cells, both at baseline and after 6 Gy irradiation, revealing an increased GSH/GSSG ratio and elevated activities of SOD, POD, and CAT enzymes in radioresistant cells compared to those in parental HCT-15 control cells. Furthermore, these changes persisted under 6 Gy irradiation.

To explore the influence of *CPT1A* overexpression on radiation resistance, we examined the GSH/GSSG ratio (Supplementary Figure 4E, F) and SOD (Supplementary Figure 4G, H), POD (Supplementary Figure 4I, J), and CAT enzyme activities (Supplementary Figure 4K) in HCT-15-25F-OE cells compared to those in control cells, showing that CPT1A overexpression restored the GSH/GSSG ratio and increased SOD and CAT enzyme activities but failed to restore POD enzyme activity.

Additionally, under 6 Gy irradiation, the GSH/GSSG ratio and SOD enzyme activity were restored in CPT1A-overexpressing cells (Supplementary Figure 4E-K).

Reduced CPT1A expression mediates radioresistance in CRC through increased expression of ROS-scavenging genes, facilitated by FOXM1

The reasons underlying the changes in SOD and CAT enzyme activities require further investigation. We examined the transcriptional and protein levels of SOD (SOD1, SOD2, and SOD3) and CAT (Figure 6A, B) and found that *CPT1A* knockout in cells increased both the mRNA and protein levels of SOD1, SOD2, and CAT, whereas the overexpression of CPT1A decreased them (Figure 6A, B). However, the function of CPT1A as a transcription factor is hitherto unreported, suggesting a potential regulatory mechanism mediated by other transcription factors. Thus, we employed a bioinformatics analysis by intersecting predicted or reported transcription factors known to regulate SOD1, SOD2, and CAT with upregulated DEGs. The Venn diagram highlights three transcription factors that met the criteria: FOXM1, LMNB1, and SAP30 (Figure 6C). FOXM1 transcription and protein levels were significantly increased in *CPT1A* knockout cells but decreased when *CPT1A* was overexpressed (Figure 6A, B). Other transcription factors showed no significant changes in protein levels (data not shown).

Additionally, we explored the correlation between FOXM1 and the downstream enzymes SOD1, SOD2, and CAT in READ and COAD. The results (Supplementary Figure 5A and B) indicate a positive correlation between FOXM1 and SOD1 as well as SOD2. Furthermore, we used hTFtarget and JASPAR to predict FOXM1 binding sites in the promoters of *SOD1*, *SOD2*, and *CAT* (Table 2). Finally, a rescue experiment was conducted by overexpressing *FOXM1* in HCT 116-NC and HCT 116-KO cells, demonstrating that downstream SOD1, SOD2, and CAT protein levels were restored by *FOXM1* overexpression (Figure 6D). In summary, the downregulation of *CPT1A* increases *FOXM1* mRNA and protein levels in CRC, promoting the transcription and translation of SOD1, SOD2, and CAT, thereby accelerating the

scavenging of ROS produced after radiation exposure and ultimately leading to radiation resistance in CRC cells (Figure 6E).

Discussion

We elucidated the role of CPT1A in CRC and the molecular mechanisms involved in mediating radiosensitivity. CPT1A is often downregulated in CRC, and low CPT1A expression can worsen OS and increase the probability of radiochemotherapy resistance. Low CPT1A expression increases FOXM1 activity, promoting the transcription and translation of downstream SOD1, SOD2, and CAT, thereby facilitating the scavenging of radiation-induced ROS. Our study establishes CPT1A as an effective biomarker to predict CRC prognosis and radiotherapy sensitivity and proposes the molecular mechanism by which it mediates radiosensitivity through the FOXM1-SOD1/SOD2/CAT axis.

CPT1A is crucial to CRC initiation and progression (Mazzarelli et al., 2007). However, its role in CRC remains unclear. CPT1A is an essential tumour suppressor. Using a weighted gene co-expression network analysis to explore hub genes in CRC development, we found that CPT1A is expressed at low levels in CRC and acts as a central anticancer gene, exhibiting excellent prognostic value(He, Zeng, & Xu, 2023). Sinomenine improves colitis-associated cancer by upregulating CPT1A(J. Zhang, Huang, Dai, & Xia, 2022). In contrast, high CPT1A expression is associated with malignancy in CRC, and its inhibition ameliorates malignant phenotypes. CPT1A-mediated fatty acid oxidation promotes CRC metastasis(Wang et al., 2018). DHP-B, a CPT1A inhibitor, disrupts CPT1A-VDAC1 interaction in the mitochondria, increasing mitochondrial permeability and reducing oxygen consumption and energy metabolism in CRC cells(Hu et al., 2023). We observed significant downregulation of CPT1A expression in CRC, and low CPT1A expression was associated with worse prognosis and greater radiochemotherapy resistance, consistent with previous studies.

The PGC1α/CEBPB/CPT1A axis, which enhances lipid β-oxidation, increases ATP and NADPH levels and promotes cellular radiation resistance in nasopharyngeal carcinoma(Tan et al., 2018). Tan et al. also discovered an interaction between CPT1A and Rab14, which transports fatty acids into the mitochondria, thereby facilitating lipid oxidation and cell survival under irradiation(Du et al., 2019). The HER1/2-MEK-ERK1/2-CPT1A/CPT2 axis reportedly enhances cell proliferation and confers radiation resistance in breast cancer(Han et al., 2019). However, no studies have investigated the association between CPT1A and radiosensitivity in CRC. Our research revealed that CPT1A is a radiation sensitivity gene, contradicting previous literature, possibly due to differences in cancer types.

Transcriptomic sequencing revealed that CPT1A regulates multiple pathways, including the peroxisomal pathway, which is responsible for ROS scavenging. *CPT1A* knockdown upregulated FOXM1, which, in turn, stimulated the transcription and translation of crucial antioxidative enzymes, SOD1, SOD2, and CAT, thereby expediting ROS clearance. This contradicts previous findings that CPT1A overexpression accelerates ROS production by increasing fatty acid β-oxidation, thereby promoting ageing phenotypes or augmenting cancer cells' oxidative defences(Jiang et al., 2022; Joshi et al., 2020; Luo, Sun, Wang, Zhang, & Wang, 2021). Our findings diverge from those of other studies for two main reasons: first, previous research into the effects of CPT1A on ROS largely centred around mitochondria rather than the peroxisome; second, previous studies did not account for radiation, which significantly increases ROS production above cellular oxidative processes.

We identified FOXM1 as a key regulator connecting CPT1A to ROS scavenging in CRC, exhibiting an inverse correlation with both CPT1A and ROS levels. FOXM1 is an essential transcription factor in intracellular redox, specifically in regulating the redox state of malignant mesothelioma cells(Cunniff, Wozniak, Sweeney, DeCosta, & Heintz, 2014). FOXM1-dependent fatty acid oxidation-mediated ROS modulation is a

cell-intrinsic drug resistance mechanism in cancer stem cells(Choi et al., 2020). *FOXM1* knockdown increases intracellular ROS levels and decreases the transcription levels of SOD2, CAT, PRDX, and GPX2(Smirnov et al., 2016). Overall, our findings align with existing literature, highlighting the crucial role of FOXM1 in orchestrating the interplay between CPT1A and ROS homoeostasis. We further revealed that FOXM1 participates in the transcriptional regulation of SOD1.

Our study has some limitations. We only conducted radiosensitivity investigations of CPT1A in nude mice, which only demonstrated its regulatory role in CRC cell radiosensitivity. It remains unclear whether CPT1A can regulate the radiosensitivity of the entire tumour microenvironment in immunocompetent mice. Additionally, FOXM1 primarily localises to the nucleus, whereas CPT1A is a cytoplasmic protein; there is no known physiological basis for their co-localisation. Therefore, the specific mechanism through which CPT1A regulates FOXM1 expression requires further investigation. The reasons for the decreased expression of CPT1A in tumour cells remain unclear. Future studies should explore this in greater detail.

Conclusions

We elucidated a novel molecular pathway underlying radioresistance in CRC cells, whereby downregulation of CPT1A induces an increase in both mRNA and protein levels of FOXM1. This elevation subsequently augments the transcription and translation of SOD1, SOD2, and CAT, thereby expediting radiation-induced ROS clearance. The resulting enhanced ROS scavenging confers a marked increase in cellular resistance to radiotherapy. Our findings highlight that the CPT1A-FOXM1-SOD/CAT axis is a critical contributor to radioresistance in CRC, offering new perspectives to unravel the intricacies of radioresistance mechanisms and potentially guiding innovative therapeutic interventions to overcome this challenge.

Data Availability Statement

Raw mRNA expression profiles and clinical features of the GSE9348, GSE20916, GSE37364, GSE44076, GSE68468 and GSE110223 datasets are available in the GEO database (http://www.ncbi.nlm.nih.gov/geo/). The raw mRNA expression profiles of rectal and colon cancer patients in the TCGA database are available ualcan database (ualcan.path.uab.edu/). The mRNA sequencing data that support the findings of this study are available from the corresponding author upon reasonable request.

Funding statement

This research project was supported by the National Natural Science Foundation of China (No. 82273564, 32370139, 32300085and 32070118), Key Science &Technology Brainstorm Project of Guangzhou (No. 202206010045), Project of Administration of Traditional Chinese Medicine of Guangdong Province of China (No.20221269).

Conflict of interest disclosure

The authors have no conflicts of interest to declare.

Ethics approval statement

All tumour tissues from patients were gifted by the Department of Pathology, Nanfang Hospital of Southern Medical University. The Specimen collection was approved by the Ethics Committee of Nanfang Hospital, Southern Medical University (Guangzhou, China). All animal experiments were approved by the Institutional Animal Care and Use Committee of Nanfang Hospital, Southern Medical University (Guangzhou, China).

Acknowledgements

We would like to thank Editage (www.editage.cn) for English language editing.

References

542 Alimardan, Z., Abbasi, M., Hasanzadeh, F., Aghaei, M., Khodarahmi, G., & Kashfi, K. (2023). Heat
543 shock proteins and cancer: The FoxM1 connection. *Biochem Pharmacol, 211*, 115505.
544 doi:10.1016/j.bcp.2023.115505
545 Bhattacharyya, A., Chattopadhyay, R., Mitra, S., & Crowe, S. E. (2014). Oxidative stress: an essential
546 factor in the pathogenesis of gastrointestinal mucosal diseases. *Physiol Rev, 94*(2), 329-354.
547 doi:10.1152/physrev.00040.2012
548 Cercek, A., Roxburgh, C. S. D., Strombom, P., Smith, J. J., Temple, L. K. F., Nash, G. M., . . . Weiser,
549 M. R. (2018). Adoption of Total Neoadjuvant Therapy for Locally Advanced Rectal Cancer.
550 *JAMA Oncol, 4*(6), e180071. doi:10.1001/jamaoncol.2018.0071
551 Cervantes, A., Adam, R., Rosello, S., Arnold, D., Normanno, N., Taieb, J., . . .
552 clinicalguidelines@esmo.org, E. G. C. E. a. (2023). Metastatic colorectal cancer: ESMO
553 Clinical Practice Guideline for diagnosis, treatment and follow-up. *Ann Oncol, 34*(1), 10-32.
554 doi:10.1016/j.annonc.2022.10.003
555 Chandrashekar, D. S., Karthikeyan, S. K., Korla, P. K., Patel, H., Shovon, A. R., Athar, M., . . .
556 Varambally, S. (2022). UALCAN: An update to the integrated cancer data analysis platform.
557 *Neoplasia, 25*, 18-27. doi:10.1016/j.neo.2022.01.001
558 Chio, I. I. C., & Tuveson, D. A. (2017). ROS in Cancer: The Burning Question. *Trends Mol Med, 23*(5),
559 411-429. doi:10.1016/j.molmed.2017.03.004
560 Choi, H. J., Jhe, Y. L., Kim, J., Lim, J. Y., Lee, J. E., Shin, M. K., & Cheong, J. H. (2020). FoxM1-
561 dependent and fatty acid oxidation-mediated ROS modulation is a cell-intrinsic drug
562 resistance mechanism in cancer stem-like cells. *Redox Biol, 36*, 101589.
563 doi:10.1016/j.redox.2020.101589
564 Cunniff, B., Wozniak, A. N., Sweeney, P., DeCosta, K., & Heintz, N. H. (2014). Peroxiredoxin 3 levels
565 regulate a mitochondrial redox setpoint in malignant mesothelioma cells. *Redox Biol, 3*, 79-
566 87. doi:10.1016/j.redox.2014.11.003
567 Du, Q., Tan, Z., Shi, F., Tang, M., Xie, L., Zhao, L., . . . Cao, Y. (2019). PGC1α/CEBPB/CPT1A axis
568 promotes radiation resistance of nasopharyngeal carcinoma through activating fatty acid
569 oxidation. *Cancer Sci, 110*(6), 2050-2062. doi:10.1111/cas.14011
570 Glasauer, A., & Chandel, N. S. (2014). Targeting antioxidants for cancer therapy. *Biochem Pharmacol,*
571 *92*(1), 90-101. doi:10.1016/j.bcp.2014.07.017

572 Glynne-Jones, R., Wyrwicz, L., Tiret, E., Brown, G., Rodel, C., Cervantes, A., & Arnold, D. (2017).
573 Rectal cancer: ESMO Clinical Practice Guidelines for diagnosis, treatment and follow-up. *Ann*
574 *Oncol, 28*(suppl_4), iv22-iv40. doi:10.1093/annonc/mdx224
575 Han, S., Wei, R., Zhang, X., Jiang, N., Fan, M., Huang, J. H., . . . Li, J. J. (2019). CPT1A/2-Mediated
576 FAO Enhancement-A Metabolic Target in Radioresistant Breast Cancer. *Front Oncol, 9*, 1201.
577 doi:10.3389/fonc.2019.01201
578 Hecht, F., Zocchi, M., Alimohammadi, F., & Harris, I. S. (2024). Regulation of antioxidants in cancer.
579 *Mol Cell, 84*(1), 23-33. doi:10.1016/j.molcel.2023.11.001
580 Hu, A., Wang, H., Xu, Q., Pan, Y., Jiang, Z., Li, S., . . . Wang, X. (2023). A novel CPT1A covalent
581 inhibitor modulates fatty acid oxidation and CPT1A-VDAC1 axis with therapeutic potential
582 for colorectal cancer. *Redox Biol, 68*, 102959. doi:10.1016/j.redox.2023.102959
583 Jiang, N., Xing, B., Peng, R., Shang, J., Wu, B., Xiao, P., . . . Lu, H. (2022). Inhibition of Cpt1a
584 alleviates oxidative stress-induced chondrocyte senescence via regulating mitochondrial
585 dysfunction and activating mitophagy. *Mech Ageing Dev, 205*, 111688.
586 doi:10.1016/j.mad.2022.111688
587 Joshi, M., Kim, J., D'Alessandro, A., Monk, E., Bruce, K., Elajaili, H., . . . Schlaepfer, I. R. (2020).
588 CPT1A Over-Expression Increases Reactive Oxygen Species in the Mitochondria and
589 Promotes Antioxidant Defenses in Prostate Cancer. *Cancers (Basel), 12*(11).
590 doi:10.3390/cancers12113431
591 Kalathil, D., John, S., & Nair, A. S. (2020). FOXM1 and Cancer: Faulty Cellular Signaling Derails
592 Homeostasis. *Front Oncol, 10*, 626836. doi:10.3389/fonc.2020.626836
593 Khan, M. A., Khan, P., Ahmad, A., Fatima, M., & Nasser, M. W. (2023). FOXM1: A small fox that
594 makes more tracks for cancer progression and metastasis. *Semin Cancer Biol, 92*, 1-15.
595 doi:10.1016/j.semcancer.2023.03.007
596 Kwon, Y. S., Lee, M. G., Baek, J., Kim, N. Y., Jang, H., & Kim, S. (2021). Acyl-CoA synthetase-4
597 mediates radioresistance of breast cancer cells by regulating FOXM1. *Biochem Pharmacol,*
598 *192*, 114718. doi:10.1016/j.bcp.2021.114718
599 Li, Z., Liu, X., Yu, H., Wang, S., Zhao, S., & Jiang, G. (2022). USP21 regulates Hippo signaling to
600 promote radioresistance by deubiquitinating FOXM1 in cervical cancer. *Hum Cell, 35*(1), 333-
601 347. doi:10.1007/s13577-021-00650-9

602 Liu, N., Cui, W., Jiang, X., Zhang, Z., Gnosa, S., Ali, Z., . . . Sun, X. F. (2019). The Critical Role of
603 Dysregulated RhoB Signaling Pathway in Radioresistance of Colorectal Cancer. *Int J Radiat*
604 *Oncol Biol Phys, 104*(5), 1153-1164. doi:10.1016/j.ijrobp.2019.04.021
605 Liu, S., Wang, Z., Zhu, R., Wang, F., Cheng, Y., & Liu, Y. (2021). Three Differential Expression
606 Analysis Methods for RNA Sequencing: limma, EdgeR, DESeq2. *J Vis Exp*(175).
607 doi:10.3791/62528
608 Luo, X., Sun, D., Wang, Y., Zhang, F., & Wang, Y. (2021). Cpt1a promoted ROS-induced oxidative
609 stress and inflammation in liver injury via the Nrf2/HO-1 and NLRP3 inflammasome
610 signaling pathway. *Can J Physiol Pharmacol, 99*(5), 468-477. doi:10.1139/cjpp-2020-0165
611 Mazzarelli, P., Pucci, S., Bonanno, E., Sesti, F., Calvani, M., & Spagnoli, L. G. (2007). Carnitine
612 palmitoyltransferase I in human carcinomas: a novel role in histone deacetylation? *Cancer*
613 *Biol Ther, 6*(10), 1606-1613. doi:10.4161/cbt.6.10.4742
614 Melone, M. A. B., Valentino, A., Margarucci, S., Galderisi, U., Giordano, A., & Peluso, G. (2018). The
615 carnitine system and cancer metabolic plasticity. *Cell Death Dis, 9*(2), 228.
616 doi:10.1038/s41419-018-0313-7
617 Pal, S., Kozono, D., Yang, X., Fendler, W., Fitts, W., Ni, J., . . . Haas-Kogan, D. A. (2018). Dual HDAC
618 and PI3K Inhibition Abrogates NFκB- and FOXM1-Mediated DNA Damage Response to
619 Radiosensitize Pediatric High-Grade Gliomas. *Cancer Res, 78*(14), 4007-4021.
620 doi:10.1158/0008-5472.can-17-3691
621 Palma, F. R., Gantner, B. N., Sakiyama, M. J., Kayzuka, C., Shukla, S., Lacchini, R., . . . Bonini, M. G.
622 (2023). ROS production by mitochondria: function or dysfunction? *Oncogene*.
623 doi:10.1038/s41388-023-02907-z
624 Qu, Q., Zeng, F., Liu, X., Wang, Q. J., & Deng, F. (2016). Fatty acid oxidation and carnitine
625 palmitoyltransferase I: emerging therapeutic targets in cancer. *Cell Death Dis, 7*(5), e2226.
626 doi:10.1038/cddis.2016.132
627 Rauluseviciute, I., Riudavets-Puig, R., Blanc-Mathieu, R., Castro-Mondragon, J. A., Ferenc, K.,
628 Kumar, V., . . . Mathelier, A. (2024). JASPAR 2024: 20th anniversary of the open-access
629 database of transcription factor binding profiles. *Nucleic Acids Res, 52*(D1), D174-D182.
630 doi:10.1093/nar/gkad1059
631 Schlaepfer, I. R., & Joshi, M. (2020). CPT1A-mediated Fat Oxidation, Mechanisms, and Therapeutic

632 Potential. *Endocrinology, 161*(2). doi:10.1210/endocr/bqz046

633 Shah, R., Ibis, B., Kashyap, M., & Boussiotis, V. A. (2023). The role of ROS in tumour infiltrating
634 immune cells and cancer immunotherapy. *Metabolism, 151*, 155747.
635 doi:10.1016/j.metabol.2023.155747

636 Siegel, R. L., Wagle, N. S., Cercek, A., Smith, R. A., & Jemal, A. (2023). Colorectal cancer statistics,
637 2023. *CA Cancer J Clin, 73*(3), 233-254. doi:10.3322/caac.21772

638 Skvortsova, I., Debbage, P., Kumar, V., & Skvortsov, S. (2015). Radiation resistance: Cancer stem cells
639 (CSCs) and their enigmatic pro-survival signaling. *Semin Cancer Biol, 35*, 39-44.
640 doi:10.1016/j.semcancer.2015.09.009

641 Smirnov, A., Panatta, E., Lena, A., Castiglia, D., Di Daniele, N., Melino, G., & Candi, E. (2016).
642 FOXM1 regulates proliferation, senescence and oxidative stress in keratinocytes and cancer
643 cells. *Aging (Albany NY), 8*(7), 1384-1397. doi:10.18632/aging.100988

644 Takeshita, H., Yoshida, R., Inoue, J., Ishikawa, K., Shinohara, K., Hirayama, M., . . . Nakayama, H.
645 (2023). FOXM1-Mediated Regulation of Reactive Oxygen Species and Radioresistance in
646 Oral Squamous Cell Carcinoma Cells. *Lab Invest, 103*(5), 100060.
647 doi:10.1016/j.labinv.2022.100060

648 Tan, Z., Xiao, L., Tang, M., Bai, F., Li, J., Li, L., . . . Cao, Y. (2018). Targeting CPT1A-mediated fatty
649 acid oxidation sensitizes nasopharyngeal carcinoma to radiation therapy. *Theranostics, 8*(9),
650 2329-2347. doi:10.7150/thno.21451

651 Tang, Z., Kang, B., Li, C., Chen, T., & Zhang, Z. (2019). GEPIA2: an enhanced web server for large-
652 scale expression profiling and interactive analysis. *Nucleic Acids Res, 47*(W1), W556-W560.
653 doi:10.1093/nar/gkz430

654 Tong Chen, Y.-X. L., Luqi Huang. (2022). ImageGP: An easy-to-use data visulization web server for
655 scientific researchers. *iMeta, 1*(1), e5.

656 Wang, Y. N., Zeng, Z. L., Lu, J., Wang, Y., Liu, Z. X., He, M. M., . . . Xu, R. H. (2018). CPT1A-
657 mediated fatty acid oxidation promotes colorectal cancer cell metastasis by inhibiting anoikis.
658 *Oncogene, 37*(46), 6025-6040. doi:10.1038/s41388-018-0384-z

659 Wu, T., Hu, E., Xu, S., Chen, M., Guo, P., Dai, Z., . . . Yu, G. (2021). clusterProfiler 4.0: A universal
660 enrichment tool for interpreting omics data. *Innovation (Camb), 2*(3), 100141.
661 doi:10.1016/j.xinn.2021.100141

662 Xiu, G., Sui, X., Wang, Y., & Zhang, Z. (2018). FOXM1 regulates radiosensitivity of lung cancer cell
663 partly by upregulating KIF20A. *Eur J Pharmacol, 833*, 79-85.
664 doi:10.1016/j.ejphar.2018.04.021
665 Xu, Z., Wang, J., & Wang, G. (2023). Weighted gene co-expression network analysis for hub genes in
666 colorectal cancer. *Pharmacol Rep*. doi:10.1007/s43440-023-00561-6
667 Yu, L., Guo, Q., Luo, Z., Wang, Y., Weng, J., Chen, Y., . . . Zhang, Y. (2022). TXN inhibitor impedes
668 radioresistance of colorectal cancer cells with decreased ALDH1L2 expression via TXN/NF-
669 kappaB signaling pathway. *Br J Cancer, 127*(4), 637-648. doi:10.1038/s41416-022-01835-1
670 Zhang, J., Huang, D., Dai, Y., & Xia, Y. F. (2022). Sinomenine Ameliorates Colitis-Associated Cancer
671 by Modulating Lipid Metabolism via Enhancing CPT1A Expression. *Metabolites, 12*(10).
672 doi:10.3390/metabo12100946
673 Zhang, Q., Liu, W., Zhang, H. M., Xie, G. Y., Miao, Y. R., Xia, M., & Guo, A. Y. (2020). hTFtarget: A
674 Comprehensive Database for Regulations of Human Transcription Factors and Their Targets.
675 *Genomics Proteomics Bioinformatics, 18*(2), 120-128. doi:10.1016/j.gpb.2019.09.006
676 Alimardan, Z., Abbasi, M., Hasanzadeh, F., Aghaei, M., Khodarahmi, G., & Kashfi, K. (2023). Heat
677 shock proteins and cancer: The FoxM1 connection. *Biochem Pharmacol, 211*, 115505.
678 doi:10.1016/j.bcp.2023.115505
679 Bhattacharyya, A., Chattopadhyay, R., Mitra, S., & Crowe, S. E. (2014). Oxidative stress: an essential
680 factor in the pathogenesis of gastrointestinal mucosal diseases. *Physiol Rev, 94*(2), 329-354.
681 doi:10.1152/physrev.00040.2012
682 Cercek, A., Roxburgh, C. S. D., Strombom, P., Smith, J. J., Temple, L. K. F., Nash, G. M., . . . Weiser,
683 M. R. (2018). Adoption of Total Neoadjuvant Therapy for Locally Advanced Rectal Cancer.
684 *JAMA Oncol, 4*(6), e180071. doi:10.1001/jamaoncol.2018.0071
685 Cervantes, A., Adam, R., Rosello, S., Arnold, D., Normanno, N., Taieb, J., . . .
686 clinicalguidelines@esmo.org, E. G. C. E. a. (2023). Metastatic colorectal cancer: ESMO
687 Clinical Practice Guideline for diagnosis, treatment and follow-up. *Ann Oncol, 34*(1), 10-32.
688 doi:10.1016/j.annonc.2022.10.003
689 Chandrashekar, D. S., Karthikeyan, S. K., Korla, P. K., Patel, H., Shovon, A. R., Athar, M., . . .
690 Varambally, S. (2022). UALCAN: An update to the integrated cancer data analysis platform.
691 *Neoplasia, 25*, 18-27. doi:10.1016/j.neo.2022.01.001

692 Chio, I. I. C., & Tuveson, D. A. (2017). ROS in Cancer: The Burning Question. *Trends Mol Med, 23*(5),
693 411-429. doi:10.1016/j.molmed.2017.03.004
694 Choi, H. J., Jhe, Y. L., Kim, J., Lim, J. Y., Lee, J. E., Shin, M. K., & Cheong, J. H. (2020). FoxM1-
695 dependent and fatty acid oxidation-mediated ROS modulation is a cell-intrinsic drug
696 resistance mechanism in cancer stem-like cells. *Redox Biol, 36*, 101589.
697 doi:10.1016/j.redox.2020.101589
698 Cunniff, B., Wozniak, A. N., Sweeney, P., DeCosta, K., & Heintz, N. H. (2014). Peroxiredoxin 3 levels
699 regulate a mitochondrial redox setpoint in malignant mesothelioma cells. *Redox Biol, 3*, 79-
700 87. doi:10.1016/j.redox.2014.11.003
701 Du, Q., Tan, Z., Shi, F., Tang, M., Xie, L., Zhao, L., . . . Cao, Y. (2019). PGC1α/CEBPB/CPT1A axis
702 promotes radiation resistance of nasopharyngeal carcinoma through activating fatty acid
703 oxidation. *Cancer Sci, 110*(6), 2050-2062. doi:10.1111/cas.14011
704 Glasauer, A., & Chandel, N. S. (2014). Targeting antioxidants for cancer therapy. *Biochem Pharmacol,*
705 *92*(1), 90-101. doi:10.1016/j.bcp.2014.07.017
706 Glynne-Jones, R., Wyrwicz, L., Tiret, E., Brown, G., Rodel, C., Cervantes, A., & Arnold, D. (2017).
707 Rectal cancer: ESMO Clinical Practice Guidelines for diagnosis, treatment and follow-up. *Ann*
708 *Oncol, 28*(suppl_4), iv22-iv40. doi:10.1093/annonc/mdx224
709 Han, S., Wei, R., Zhang, X., Jiang, N., Fan, M., Huang, J. H., . . . Li, J. J. (2019). CPT1A/2-Mediated
710 FAO Enhancement-A Metabolic Target in Radioresistant Breast Cancer. *Front Oncol, 9*, 1201.
711 doi:10.3389/fonc.2019.01201
712 He, W., Zeng, S., & Xu, C. (2023). Controversy Surrounding Bladder-Sparing Radical Dose
713 Radiotherapy as an Alternative to Radical Cystectomy for Clinically Node-Positive
714 Nonmetastatic Bladder Cancer. *J Clin Oncol*, Jco2301920. doi:10.1200/jco.23.01920
715 Hecht, F., Zocchi, M., Alimohammadi, F., & Harris, I. S. (2024). Regulation of antioxidants in cancer.
716 *Mol Cell, 84*(1), 23-33. doi:10.1016/j.molcel.2023.11.001
717 Hu, A., Wang, H., Xu, Q., Pan, Y., Jiang, Z., Li, S., . . . Wang, X. (2023). A novel CPT1A covalent
718 inhibitor modulates fatty acid oxidation and CPT1A-VDAC1 axis with therapeutic potential
719 for colorectal cancer. *Redox Biol, 68*, 102959. doi:10.1016/j.redox.2023.102959
720 Jiang, N., Xing, B., Peng, R., Shang, J., Wu, B., Xiao, P., . . . Lu, H. (2022). Inhibition of Cpt1a
721 alleviates oxidative stress-induced chondrocyte senescence via regulating mitochondrial

722 dysfunction and activating mitophagy. *Mech Ageing Dev, 205*, 111688.
723 doi:10.1016/j.mad.2022.111688
724 Joshi, M., Kim, J., D'Alessandro, A., Monk, E., Bruce, K., Elajaili, H., . . . Schlaepfer, I. R. (2020).
725 CPT1A Over-Expression Increases Reactive Oxygen Species in the Mitochondria and
726 Promotes Antioxidant Defenses in Prostate Cancer. *Cancers (Basel), 12*(11).
727 doi:10.3390/cancers12113431
728 Kalathil, D., John, S., & Nair, A. S. (2020). FOXM1 and Cancer: Faulty Cellular Signaling Derails
729 Homeostasis. *Front Oncol, 10*, 626836. doi:10.3389/fonc.2020.626836
730 Khan, M. A., Khan, P., Ahmad, A., Fatima, M., & Nasser, M. W. (2023). FOXM1: A small fox that
731 makes more tracks for cancer progression and metastasis. *Semin Cancer Biol, 92*, 1-15.
732 doi:10.1016/j.semcancer.2023.03.007
733 Kwon, Y. S., Lee, M. G., Baek, J., Kim, N. Y., Jang, H., & Kim, S. (2021). Acyl-CoA synthetase-4
734 mediates radioresistance of breast cancer cells by regulating FOXM1. *Biochem Pharmacol,*
735 *192*, 114718. doi:10.1016/j.bcp.2021.114718
736 Li, Z., Liu, X., Yu, H., Wang, S., Zhao, S., & Jiang, G. (2022). USP21 regulates Hippo signaling to
737 promote radioresistance by deubiquitinating FOXM1 in cervical cancer. *Hum Cell, 35*(1), 333-
738 347. doi:10.1007/s13577-021-00650-9
739 Liu, N., Cui, W., Jiang, X., Zhang, Z., Gnosa, S., Ali, Z., . . . Sun, X. F. (2019). The Critical Role of
740 Dysregulated RhoB Signaling Pathway in Radioresistance of Colorectal Cancer. *Int J Radiat*
741 *Oncol Biol Phys, 104*(5), 1153-1164. doi:10.1016/j.ijrobp.2019.04.021
742 Liu, S., Wang, Z., Zhu, R., Wang, F., Cheng, Y., & Liu, Y. (2021). Three Differential Expression
743 Analysis Methods for RNA Sequencing: limma, EdgeR, DESeq2. *J Vis Exp*(175).
744 doi:10.3791/62528
745 Luo, X., Sun, D., Wang, Y., Zhang, F., & Wang, Y. (2021). Cpt1a promoted ROS-induced oxidative
746 stress and inflammation in liver injury via the Nrf2/HO-1 and NLRP3 inflammasome
747 signaling pathway. *Can J Physiol Pharmacol, 99*(5), 468-477. doi:10.1139/cjpp-2020-0165
748 Mazzarelli, P., Pucci, S., Bonanno, E., Sesti, F., Calvani, M., & Spagnoli, L. G. (2007). Carnitine
749 palmitoyltransferase I in human carcinomas: a novel role in histone deacetylation? *Cancer*
750 *Biol Ther, 6*(10), 1606-1613. doi:10.4161/cbt.6.10.4742
751 Melone, M. A. B., Valentino, A., Margarucci, S., Galderisi, U., Giordano, A., & Peluso, G. (2018). The

carnitine system and cancer metabolic plasticity. *Cell Death Dis, 9*(2), 228. doi:10.1038/s41419-018-0313-7

Pal, S., Kozono, D., Yang, X., Fendler, W., Fitts, W., Ni, J., . . . Haas-Kogan, D. A. (2018). Dual HDAC and PI3K Inhibition Abrogates NFκB- and FOXM1-Mediated DNA Damage Response to Radiosensitize Pediatric High-Grade Gliomas. *Cancer Res, 78*(14), 4007-4021. doi:10.1158/0008-5472.can-17-3691

Palma, F. R., Gantner, B. N., Sakiyama, M. J., Kayzuka, C., Shukla, S., Lacchini, R., . . . Bonini, M. G. (2023). ROS production by mitochondria: function or dysfunction? *Oncogene*. doi:10.1038/s41388-023-02907-z

Qu, Q., Zeng, F., Liu, X., Wang, Q. J., & Deng, F. (2016). Fatty acid oxidation and carnitine palmitoyltransferase I: emerging therapeutic targets in cancer. *Cell Death Dis, 7*(5), e2226. doi:10.1038/cddis.2016.132

Rauluseviciute, I., Riudavets-Puig, R., Blanc-Mathieu, R., Castro-Mondragon, J. A., Ferenc, K., Kumar, V., . . . Mathelier, A. (2024). JASPAR 2024: 20th anniversary of the open-access database of transcription factor binding profiles. *Nucleic Acids Res, 52*(D1), D174-D182. doi:10.1093/nar/gkad1059

Schlaepfer, I. R., & Joshi, M. (2020). CPT1A-mediated Fat Oxidation, Mechanisms, and Therapeutic Potential. *Endocrinology, 161*(2). doi:10.1210/endocr/bqz046

Shah, R., Ibis, B., Kashyap, M., & Boussiotis, V. A. (2023). The role of ROS in tumour infiltrating immune cells and cancer immunotherapy. *Metabolism, 151*, 155747. doi:10.1016/j.metabol.2023.155747

Siegel, R. L., Wagle, N. S., Cercek, A., Smith, R. A., & Jemal, A. (2023). Colorectal cancer statistics, 2023. *CA Cancer J Clin, 73*(3), 233-254. doi:10.3322/caac.21772

Skvortsova, I., Debbage, P., Kumar, V., & Skvortsov, S. (2015). Radiation resistance: Cancer stem cells (CSCs) and their enigmatic pro-survival signaling. *Semin Cancer Biol, 35*, 39-44. doi:10.1016/j.semcancer.2015.09.009

Smirnov, A., Panatta, E., Lena, A., Castiglia, D., Di Daniele, N., Melino, G., & Candi, E. (2016). FOXM1 regulates proliferation, senescence and oxidative stress in keratinocytes and cancer cells. *Aging (Albany NY), 8*(7), 1384-1397. doi:10.18632/aging.100988

Takeshita, H., Yoshida, R., Inoue, J., Ishikawa, K., Shinohara, K., Hirayama, M., . . . Nakayama, H.

(2023). FOXM1-Mediated Regulation of Reactive Oxygen Species and Radioresistance in Oral Squamous Cell Carcinoma Cells. *Lab Invest, 103*(5), 100060. doi:10.1016/j.labinv.2022.100060

Tan, Z., Xiao, L., Tang, M., Bai, F., Li, J., Li, L., . . . Cao, Y. (2018). Targeting CPT1A-mediated fatty acid oxidation sensitizes nasopharyngeal carcinoma to radiation therapy. *Theranostics, 8*(9), 2329-2347. doi:10.7150/thno.21451

Tang, Z., Kang, B., Li, C., Chen, T., & Zhang, Z. (2019). GEPIA2: an enhanced web server for large-scale expression profiling and interactive analysis. *Nucleic Acids Res, 47*(W1), W556-W560. doi:10.1093/nar/gkz430

Tong Chen, Y.-X. L., Luqi Huang. (2022). ImageGP: An easy-to-use data visulization web server for scientific researchers. *iMeta, 1*(1), e5.

Wang, Y. N., Zeng, Z. L., Lu, J., Wang, Y., Liu, Z. X., He, M. M., . . . Xu, R. H. (2018). CPT1A-mediated fatty acid oxidation promotes colorectal cancer cell metastasis by inhibiting anoikis. *Oncogene, 37*(46), 6025-6040. doi:10.1038/s41388-018-0384-z

Wu, T., Hu, E., Xu, S., Chen, M., Guo, P., Dai, Z., . . . Yu, G. (2021). clusterProfiler 4.0: A universal enrichment tool for interpreting omics data. *Innovation (Camb), 2*(3), 100141. doi:10.1016/j.xinn.2021.100141

Xiu, G., Sui, X., Wang, Y., & Zhang, Z. (2018). FOXM1 regulates radiosensitivity of lung cancer cell partly by upregulating KIF20A. *Eur J Pharmacol, 833*, 79-85. doi:10.1016/j.ejphar.2018.04.021

Yu, L., Guo, Q., Luo, Z., Wang, Y., Weng, J., Chen, Y., . . . Zhang, Y. (2022). TXN inhibitor impedes radioresistance of colorectal cancer cells with decreased ALDH1L2 expression via TXN/NF-kappaB signaling pathway. *Br J Cancer, 127*(4), 637-648. doi:10.1038/s41416-022-01835-1

Zhang, J., Huang, D., Dai, Y., & Xia, Y. F. (2022). Sinomenine Ameliorates Colitis-Associated Cancer by Modulating Lipid Metabolism via Enhancing CPT1A Expression. *Metabolites, 12*(10). doi:10.3390/metabo12100946

Zhang, Q., Liu, W., Zhang, H. M., Xie, G. Y., Miao, Y. R., Xia, M., & Guo, A. Y. (2020). hTFtarget: A Comprehensive Database for Regulations of Human Transcription Factors and Their Targets. *Genomics Proteomics Bioinformatics, 18*(2), 120-128. doi:10.1016/j.gpb.2019.09.006

812 **Table 1. Correlation between clinicopathological features and the expression of CPT1A in**
813 **tumor paraffin section**

Variables[1]	Categories	CPT1A			p-Value
		Low	High	Total (n)	
Age	<50	13	13	26	0.411
	≥50	20	30	50	
Gender	Male	13	18	31	0.831
	Female	20	25	45	
Histological grade[2]	Well differentiated	3	5	8	0.640
	Moderately differentiated	26	32	58	
	Poorly differentiated	4	6	10	
UICC/ AJCC Stage	Stage I	3	1	4	0.379
	Stage II	14	16	30	
	Stage III	14	24	38	
	Stage IV	2	2	4	
T-class	T1	1	1	2	0.272
	T2	3	3	6	
	T3	15	15	30	
	T4	14	24	38	
N-class	N0	18	17	35	0.189
	N1	10	16	26	
	N2	5	10	15	
M-class	M0	31	41	72	0.788
	M1	2	2	4	

814

Table 2. Potential binding site of SOD1, SOD2, CAT promoter predicted by hTFtarget and JASPAR.

TF	Target gene	Sequence Name	Start	Stop	Strand	Score	P value	Q value	Matched motif
FOXM1	SOD1	NC_000021.9:31657693-31659693	11 66	11 78	-	14.44 12	0.00000 152	0.005 99	TTTGTTTGA TTTT
FOXM1	SOD2	NC_000006.12:c159669069-159667069	11 52	11 60	+	12.68 5	0.00000 403	0.015 9	AGATGGAG T
FOXM1	CAT	NC_000011.10:34436934-34438934	14 10	14 22	+	11.33 33	0.00004 99	0.197	TCAGAGTG TTTTT

Figure legends

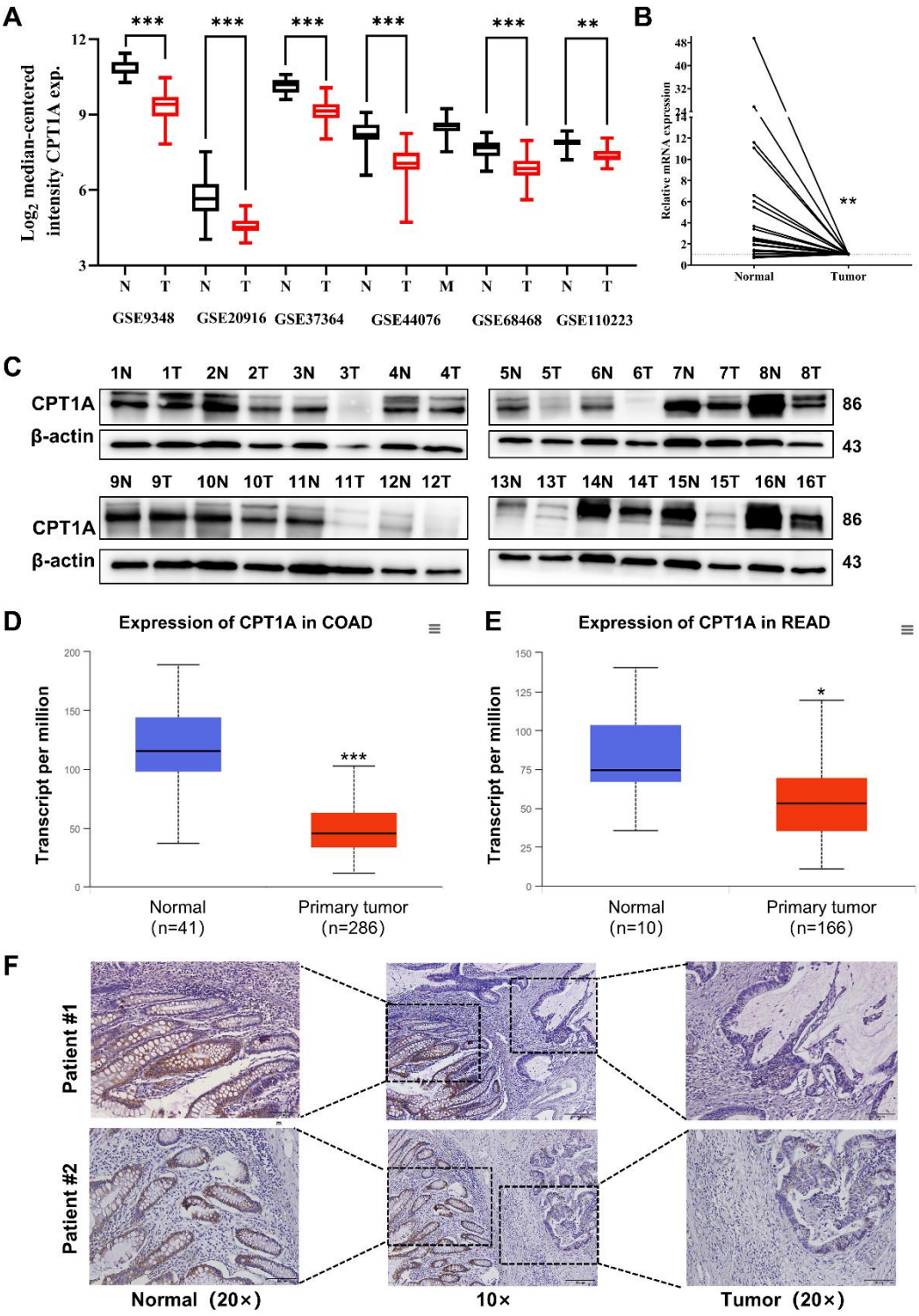

Fig 1. Aberrant CPT1A mRNA level in CRC. A. The expression of CPT1A in six GEO microarrays. B. Real-time PCR for CPT1A in 24-paired CRC and adjacent non-tumour tissues. C. Western blot for CPT1A in sixteen-paired CRC and adjacent non-tumour tissues. D. Lower CPT1A mRNA level in COAD than the normal counterparts from TCGA in ualcan database. E. Lower CPT1A mRNA level in READ than the normal counterparts from TCGA

826 in ualcan database. F. IHC assay for CPT1A in two patients. ***, $P < 0.001$, ** $P < 0.01$, * P
827 < 0.05.
828

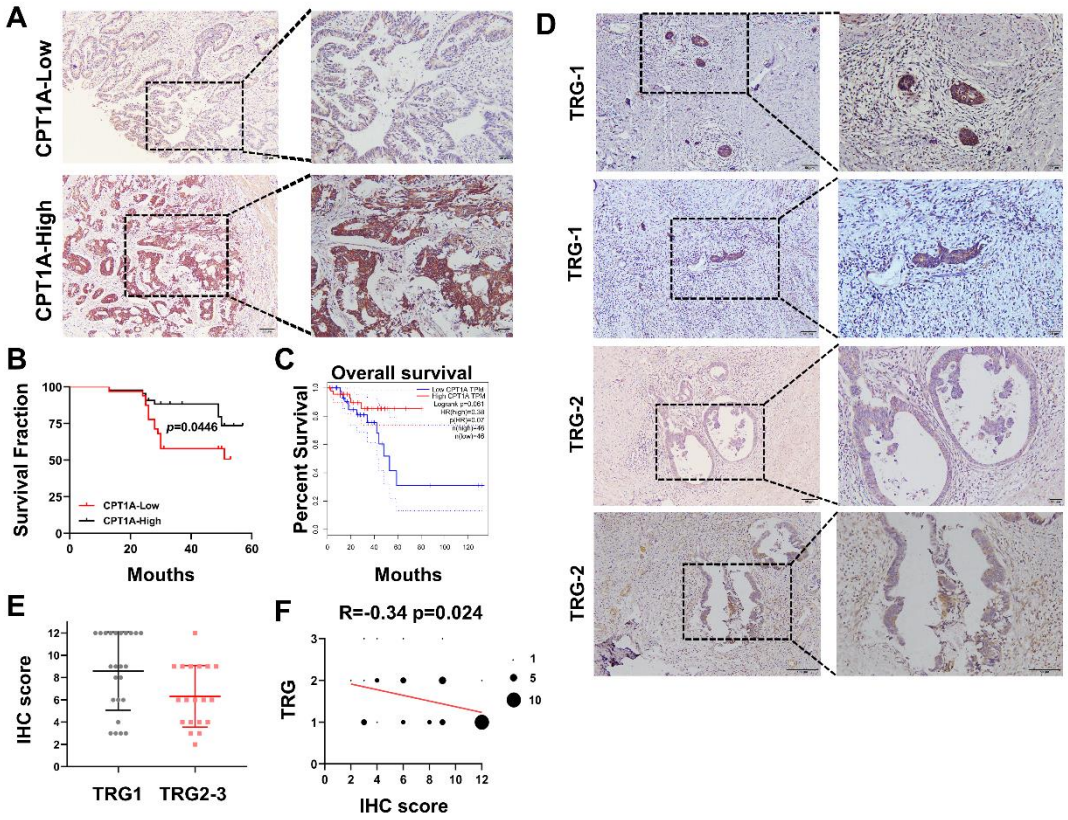

Fig 2. Correlation of CPT1A with overall survival and neoadjuvant therapy response in rectal cancer patients. A. IHC assay for CPT1A in two groups of patients, upper with low CPT1A expression and lower with high CPT1A expression. B. The Overall survival (OS) was estimated by the Kaplan-Meier method in rectal cancer patients. C. The OS was estimated by the Kaplan-Meier method in rectal cancer patients in TCGA database. D. IHC assay for CPT1A in two groups of patients, upper with TRG-1 and lower with TRG-2 (TRG means tumour regression grade, AJCC standard, 0, complete response: No remaining viable cancer cells; 1, moderate response: Only small clusters or single cancer cells remaining; 2, minimal response: Residual cancer remaining, but with predominant fibrosis). E. Dot plot showing the IHC score and TRG score of patients. F. Correlation of CPT1A with TRG score, size of dot represents the number. ***, $P < 0.001$, ** $P < 0.01$, * $P < 0.05$.

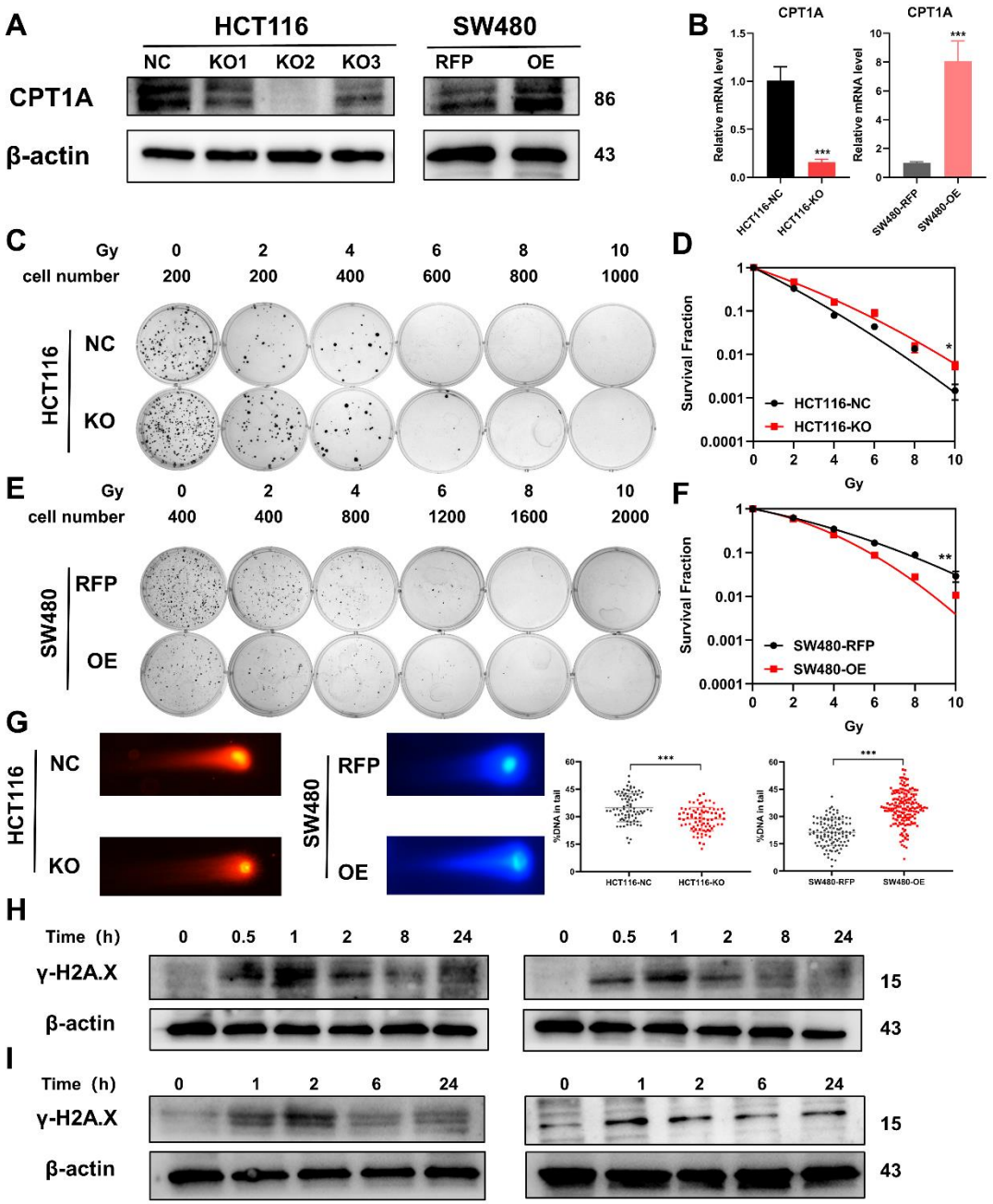

842

843 **Fig 3. Radio-sensitivity of stable knock-out or overexpression of CPT1A.** A. The protein
844 level of CPT1A in different groups of cell lines. B. The mRNA level of CPT1A in different
845 groups of cell lines. C. Colony-forming assay of HCT 116-NC and HCT 116-KO cell lines.
846 D. The map of multi-target, single-hit model. E. Colony-forming assay of SW480-RFP and
847 SW480-OE cell lines. F. The map of multi-target, single-hit model. G. Comet assay of
848 different cells. H. Protein expression of γ-H2A.X in HCT 116-NC and HCT 116-KO cell
849 lines. I. Protein expression of γ-H2A.X in SW480-RFP and SW480-OE cell lines. ***, $P <$
850 0.001, ** $P < 0.01$, * $P < 0.05$.

851

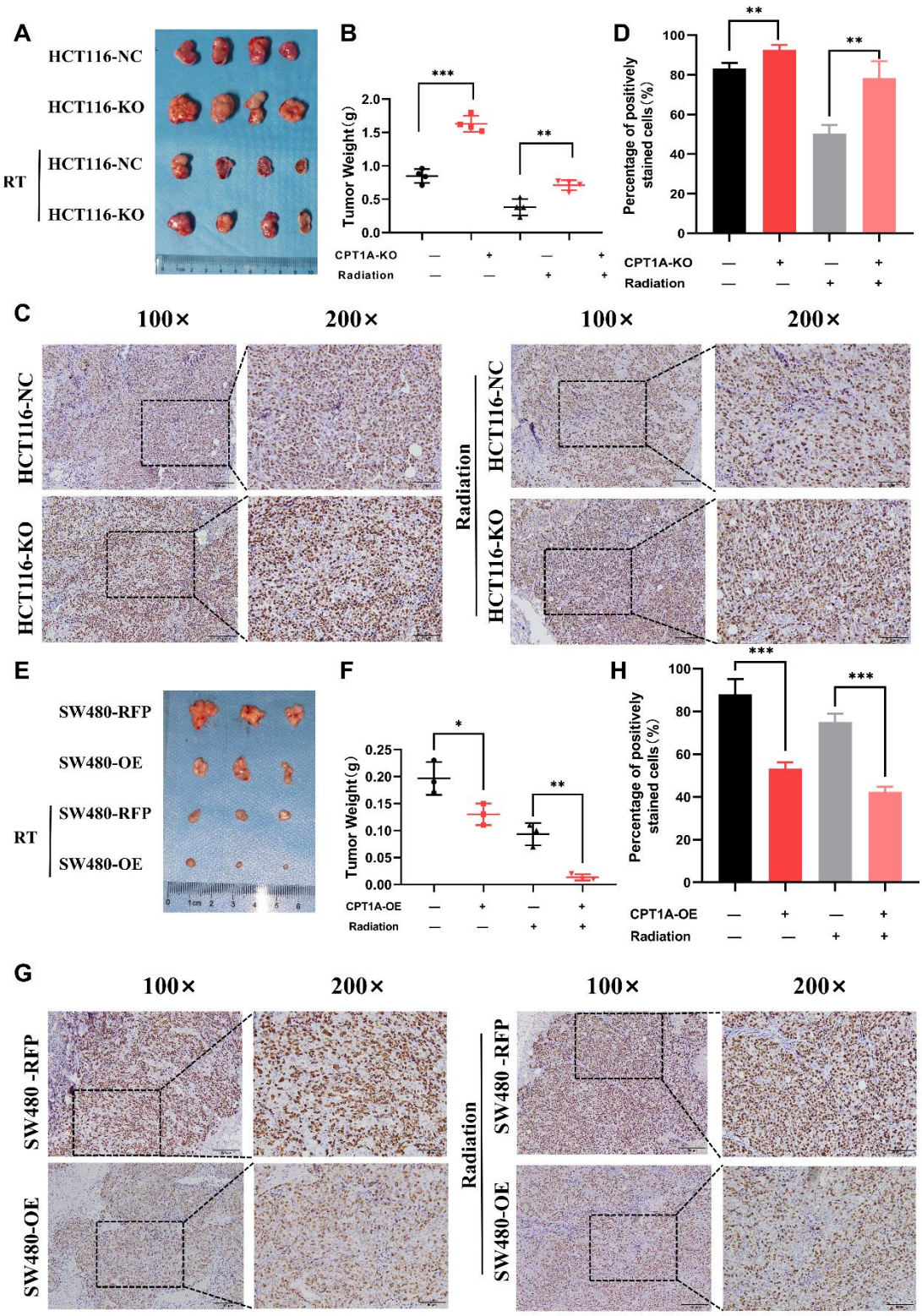

Fig 4. CPT1A inhibited proliferation and radio-resistance in nude mice. A. Image of tumours formed in nude mice, with knock out of CPT1A and radiation. B. Scattergram showing the weight of tumours. C. Immunohistochemical staining of Ki67 in tumours. D. Bar chart demonstrating the percentage of positively stained of Ki67 cells. E. Image of tumours formed in nude mice, with overexpression of CPT1A and radiation. F. Scattergram showing

858 the weight of tumours. G. Immunohistochemical staining of Ki67 in tumours. H. Bar chart
859 demonstrating the percentage of positively stained of Ki67 cells. ***, $P < 0.001$, ** $P < 0.01$,
860 * $P < 0.05$.
861

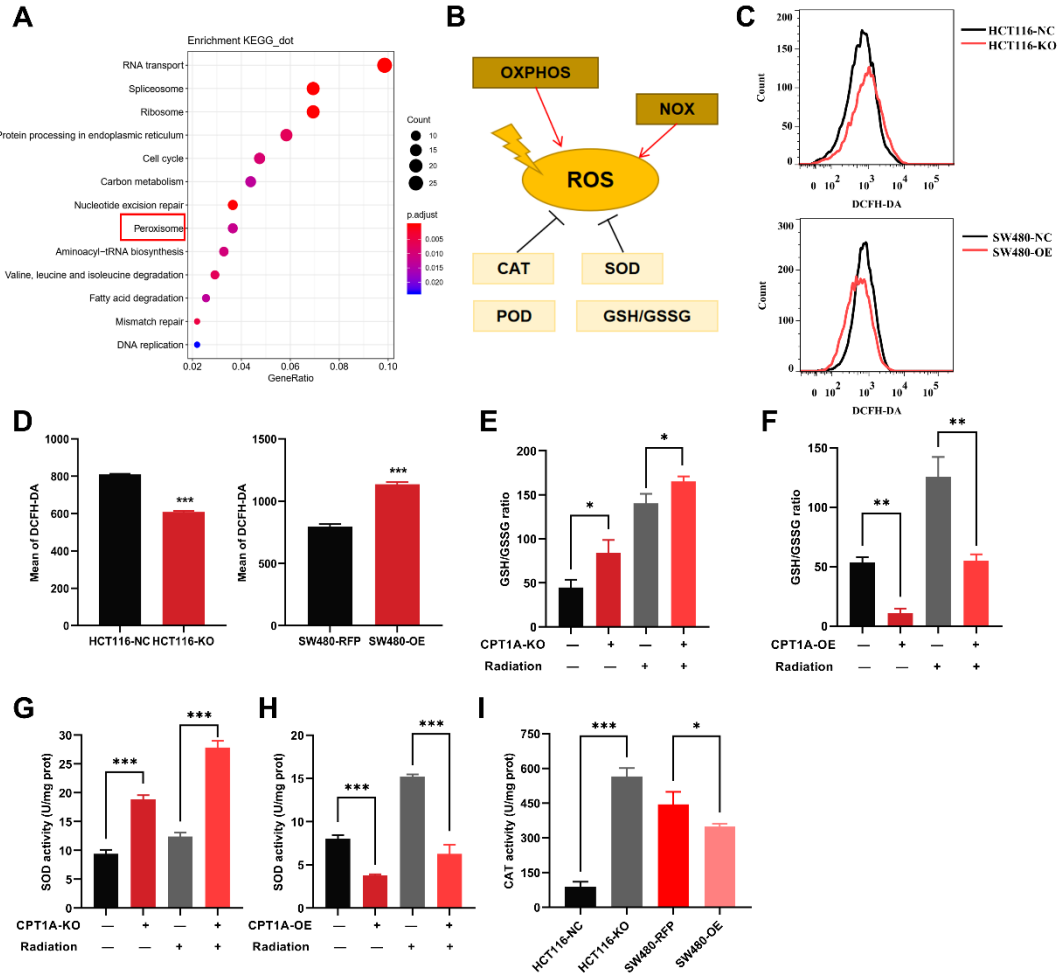

Fig 5. The effect of CPT1A on ROS related enzyme activity. A. Enriched KEGG pathway of DEGs in mRNA sequencing. B. Generation and scavenging of ROS in cell. C. ROS of HCT 116-KO cell, SW480-OE cell and their control with DCFH-DA by flow cytometry. D. Bar graph to show the mean of DCFH-DA in HCT 116-KO, HCT 116-NC cells, SW480-NC and SW480-OE cells. E. GSH / GSSG ratio measurement under CPT1A knockout and radiation. F. GSH / GSSG ratio measurement under CPT1A overexpression and radiation. G. Effect of the CPT1A knockout on SOD activity. H. Effect of the CPT1A overexpression on SOD activity. I. Effect of the CPT1A on CAT activity. ***, $P < 0.001$, ** $P < 0.01$, * $P < 0.05$.

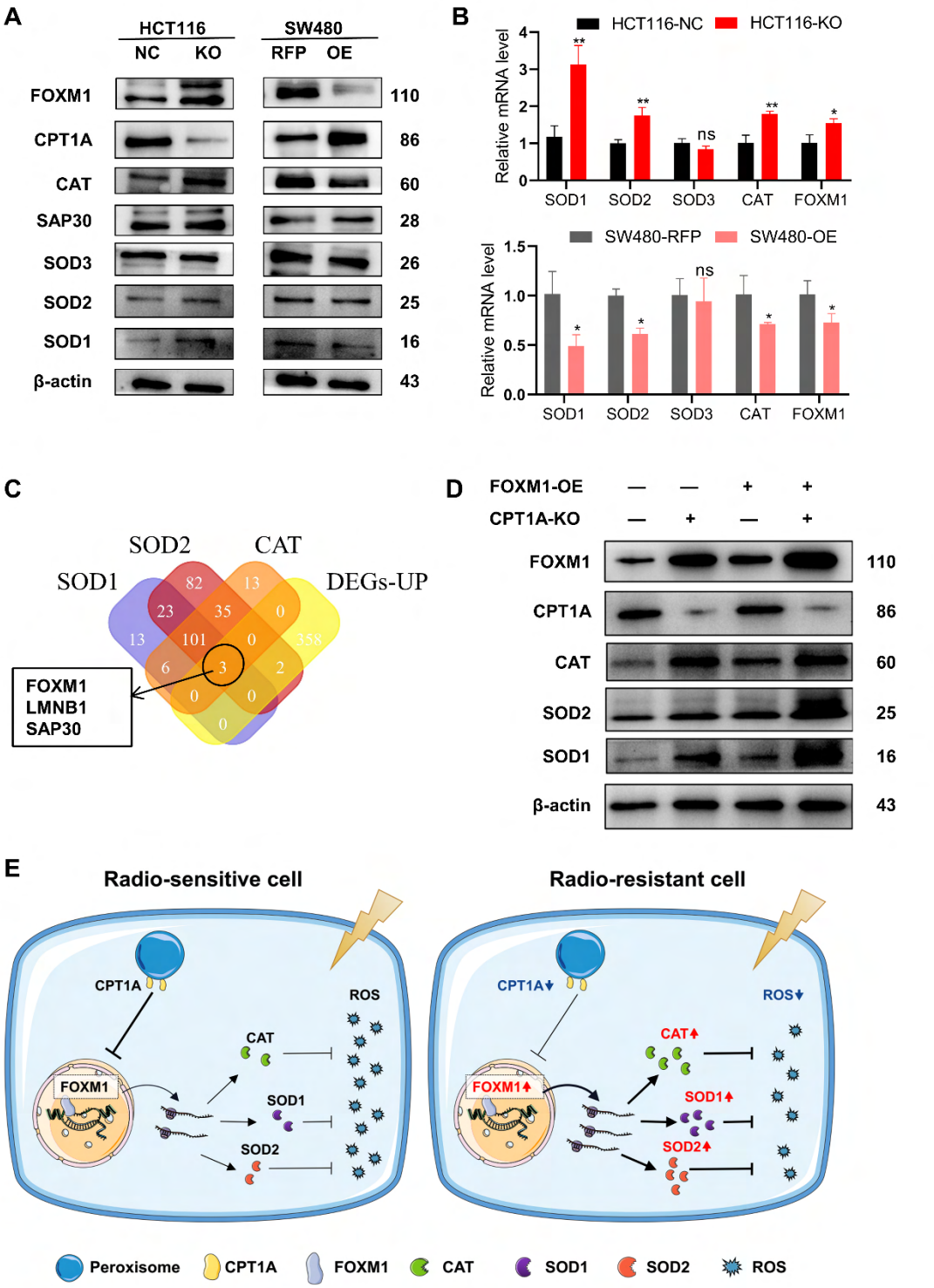

Fig 6. CPT1A increases the transcription and protein of ROS scavenge related genes by regulating the transcription factor activity of FOXM1. A.The protein level of FOXM1, CPT1A, CAT, SOD1, SOD2, SOD3 after knockout and overexpression of CPT1A. B. The mRNA level of FOXM1, CAT, SOD1, SOD2, SOD3 after knockout and overexpression of CPT1A. C. Veen map showing the potential transcription factor of SOD1, SOD2 and CAT.

879 D. The protein level of FOXM1, CPT1A, CAT, SOD1, SOD2 after overexpression of
880 FOXM1 in HCT116-CPT1AKO cells. E. Schematic diagram summarising our working
881 model, namely, decreased CPT1A promotes the transcription factor activity of FOXM1,
882 increasing the mRNA and protein level of CAT, SOD1, and SOD2, followed by increasing
883 ROS scavenge after irradiation and therefore CRC cells become radioresistance. ***, $P <$
884 0.001, ** $P < 0.01$, * $P < 0.05$.

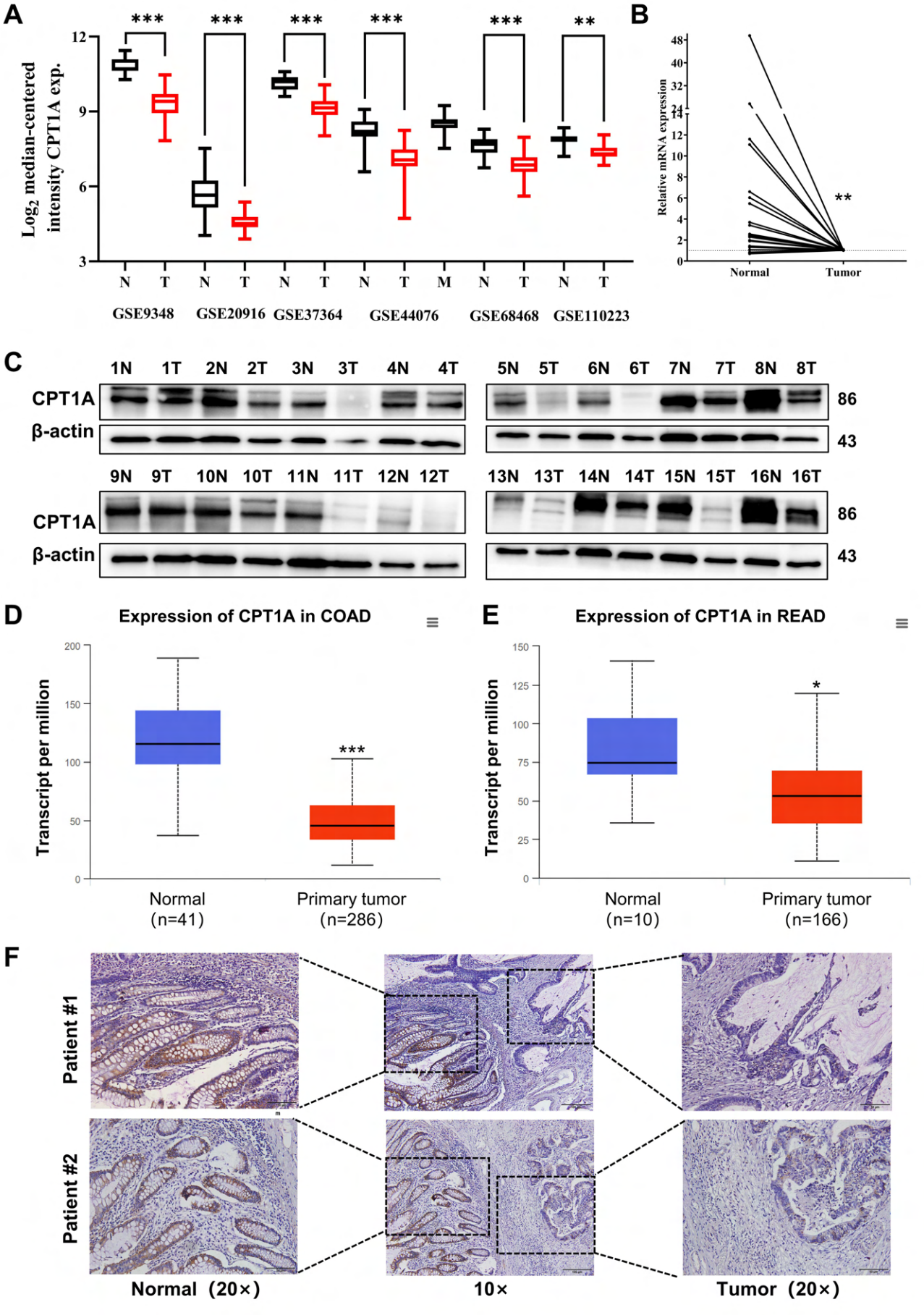
A
***
***
***
***
***
**
Log2 median-centered intensity CPT1A exp.
12
9
6
3
N T N T N T N T M N T N T
GSE9348 GSE20916 GSE37364 GSE44076 GSE68468 GSE110223
B
Relative mRNA expression
48
40
32
24
16
14
12
10
8
6
4
2
0
**
Normal
Tumor
C
1N 1T 2N 2T 3N 3T 4N 4T
5N 5T 6N 6T 7N 7T 8N 8T
CPT1A
β-actin
86
43
9N 9T 10N 10T 11N 11T 12N 12T
13N 13T 14N 14T 15N 15T 16N 16T
CPT1A
β-actin
86
43
D
Expression of CPT1A in COAD
Transcript per million
200
150
100
50
0
***
Normal
(n=41)
Primary tumor
(n=286)
E
Expression of CPT1A in READ
Transcript per million
150
125
100
75
50
25
0
*
Normal
(n=10)
Primary tumor
(n=166)
F
Patient #1
Patient #2
Normal (20×)
10×
Tumor (20×)

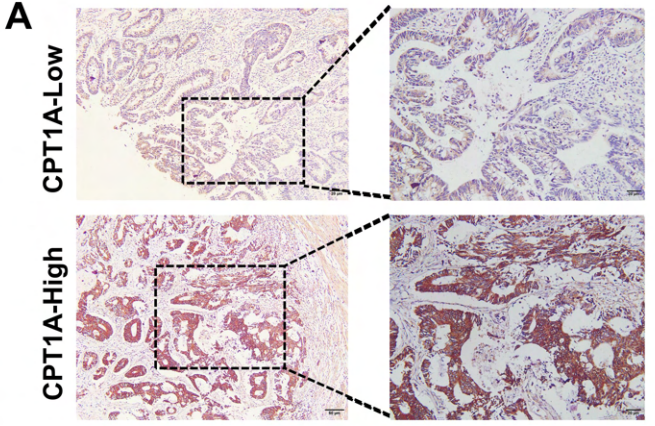
A
CPT1A-Low
CPT1A-High

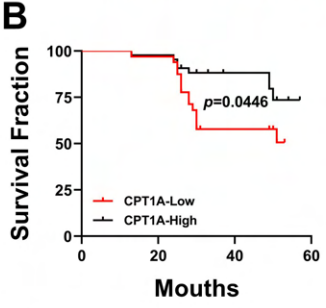
B
Survival Fraction
100
75
50
25
0
p=0.0446
CPT1A-Low
CPT1A-High
0
20
40
60
Mouths

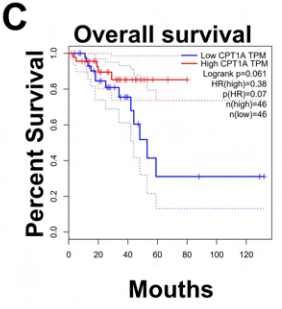
C
Overall survival
Percent Survival
Low CPT1A TPM
High CPT1A TPM
Logrank p=0.061
HR(high)=0.38
p(HR)=0.07
n(high)=46
n(low)=46
0.0
0.2
0.4
0.6
0.8
1.0
0
20
40
60
80
100
120
Mouths

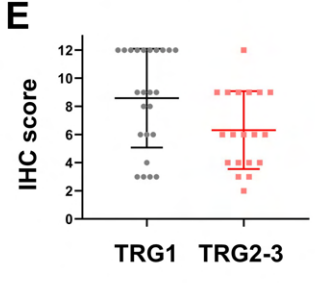
E
IHC score
12
10
8
6
4
2
0
TRG1
TRG2-3

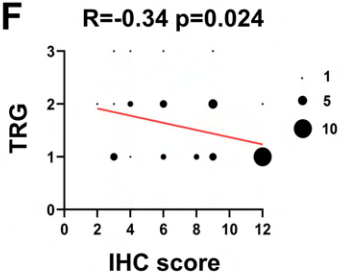
F
R=-0.34 p=0.024
TRG
3
2
1
0
0
2
4
6
8
10
12
IHC score
1
5
10

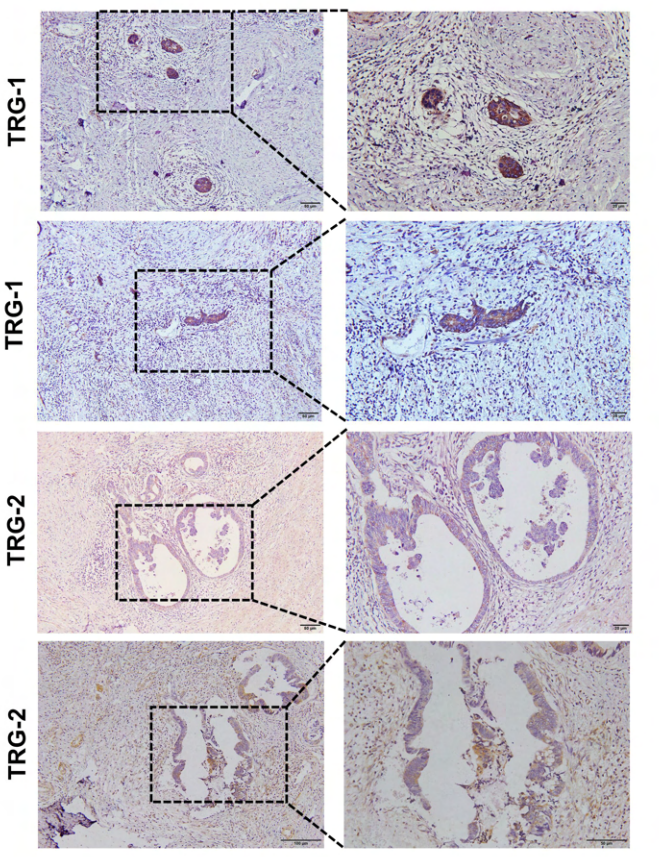
D
TRG-1
TRG-1
TRG-2
TRG-2

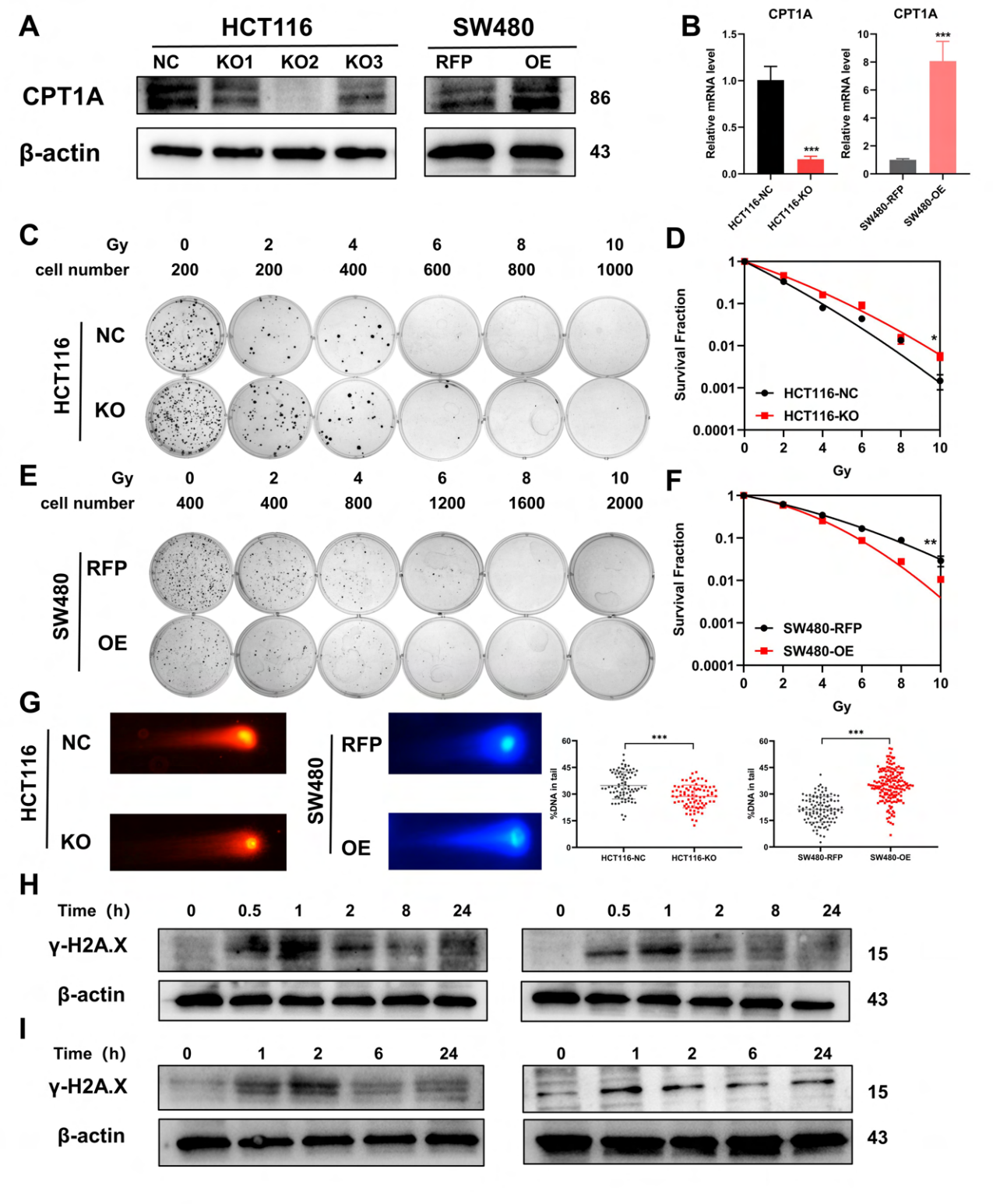
A
HCT116
SW480
NC
KO1
KO2
KO3
RFP
OE
CPT1A
β-actin
86
43
B
CPT1A
CPT1A
Relative mRNA level
Relative mRNA level
***
***
HCT116-NC
HCT116-KO
SW480-RFP
SW480-OE
C
Gy
cell number
0 2 4 6 8 10
200 200 400 600 800 1000
HCT116
NC
KO
D
Survival Fraction
HCT116-NC
HCT116-KO
*
Gy
E
Gy
cell number
0 2 4 6 8 10
400 400 800 1200 1600 2000
SW480
RFP
OE
F
Survival Fraction
SW480-RFP
SW480-OE
**
Gy
G
HCT116
NC
KO
SW480
RFP
OE
%DNA in tail
***
HCT116-NC
HCT116-KO
%DNA in tail
***
SW480-RFP
SW480-OE
H
Time (h)
0 0.5 1 2 8 24
γ-H2A.X
β-actin
15
43
I
Time (h)
0 1 2 6 24
γ-H2A.X
β-actin
15
43

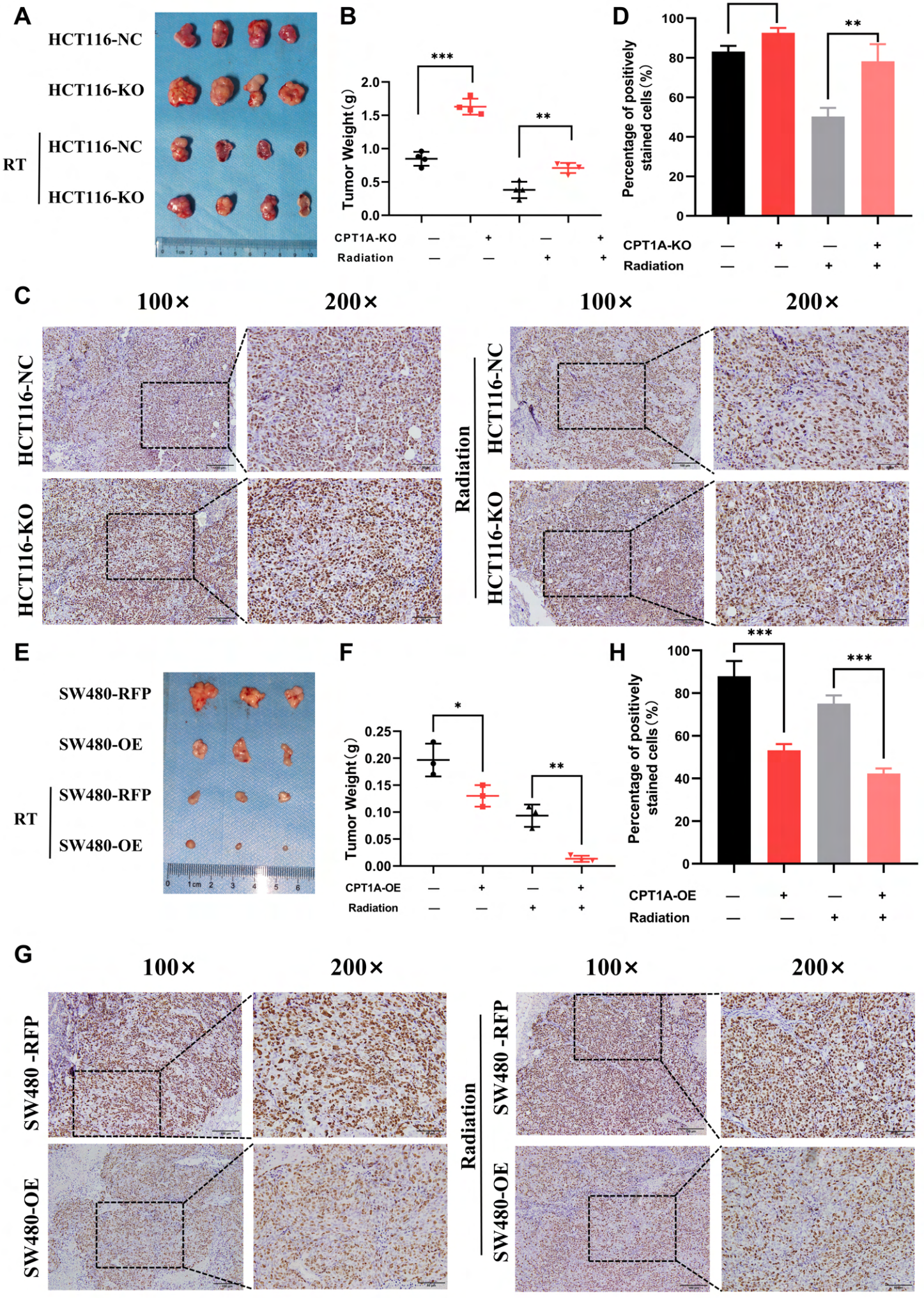
A
HCT116-NC
HCT116-KO
RT
HCT116-NC
HCT116-KO
B
Tumor Weight(g)
2.0
1.5
1.0
0.5
0.0
***
**
CPT1A-KO — + — +
Radiation — — + +
D
Percentage of positively stained cells(%)
100
80
60
40
20
0
**
**
CPT1A-KO — + — +
Radiation — — + +
C
100×
200×
100×
200×
HCT116-NC
HCT116-KO
Radiation
HCT116-NC
HCT116-KO
E
SW480-RFP
SW480-OE
RT
SW480-RFP
SW480-OE
F
Tumor Weight(g)
0.25
0.20
0.15
0.10
0.05
0.00
*
**
CPT1A-OE — + — +
Radiation — — + +
H
Percentage of positively stained cells(%)
100
80
60
40
20
0
***
***
CPT1A-OE — + — +
Radiation — — + +
G
100×
200×
100×
200×
SW480 -RFP
SW480-OE
Radiation
SW480 -RFP
SW480-OE

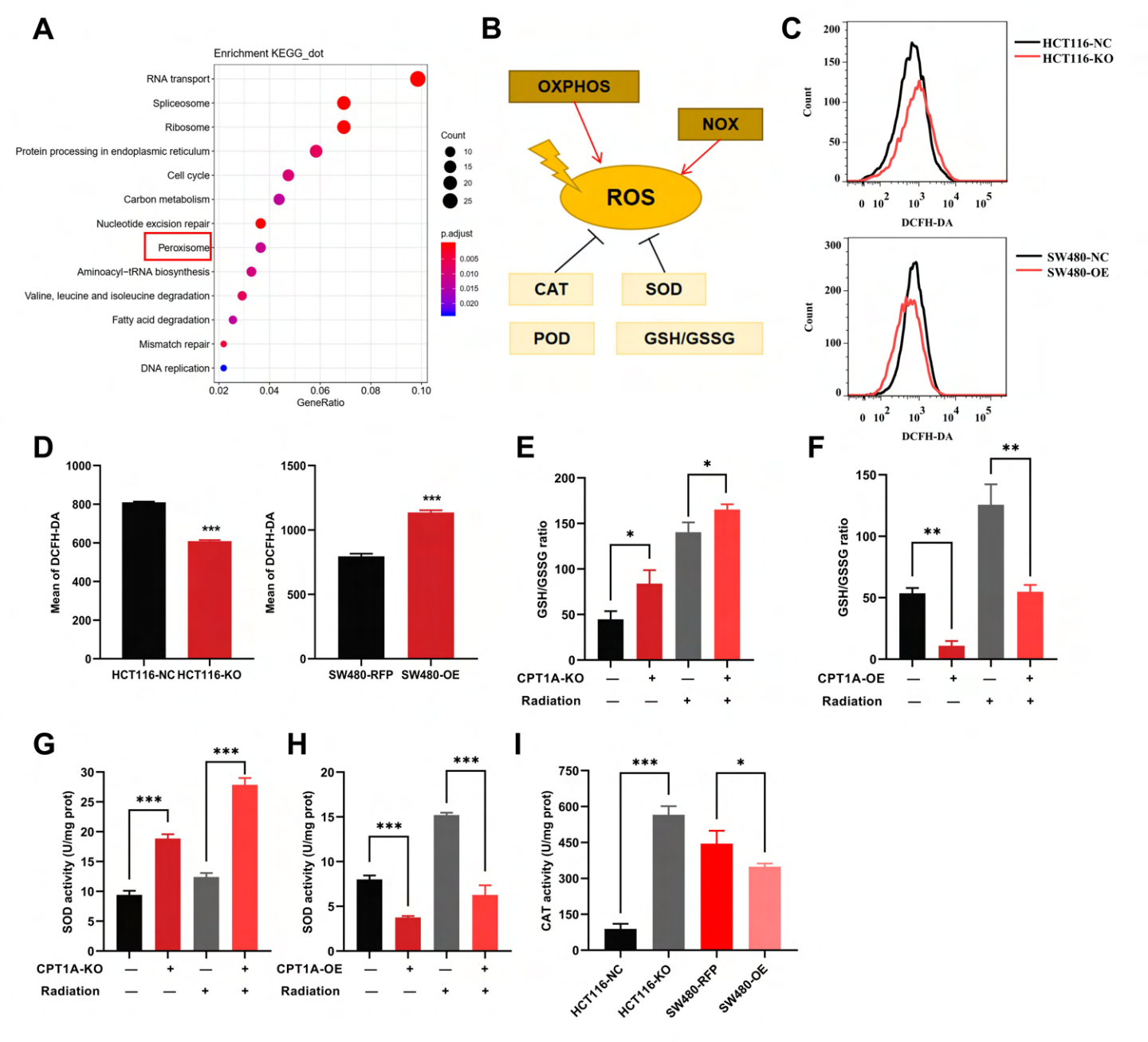
A
Enrichment KEGG_dot
RNA transport
Spliceosome
Ribosome
Protein processing in endoplasmic reticulum
Cell cycle
Carbon metabolism
Nucleotide excision repair
Peroxisome
Aminoacyl−tRNA biosynthesis
Valine, leucine and isoleucine degradation
Fatty acid degradation
Mismatch repair
DNA replication
0.02
0.04
0.06
0.08
0.10
GeneRatio
Count
10
15
20
25
p.adjust
0.005
0.010
0.015
0.020
B
OXPHOS
NOX
ROS
CAT
SOD
POD
GSH/GSSG
C
HCT116-NC
HCT116-KO
Count
DCFH-DA
SW480-NC
SW480-OE
Count
DCFH-DA
D
Mean of DCFH-DA
HCT116-NC
HCT116-KO
Mean of DCFH-DA
SW480-RFP
SW480-OE
E
GSH/GSSG ratio
CPT1A-KO
Radiation
F
GSH/GSSG ratio
CPT1A-OE
Radiation
G
SOD activity (U/mg prot)
CPT1A-KO
Radiation
H
SOD activity (U/mg prot)
CPT1A-OE
Radiation
I
CAT activity (U/mg prot)
HCT116-NC
HCT116-KO
SW480-RFP
SW480-OE

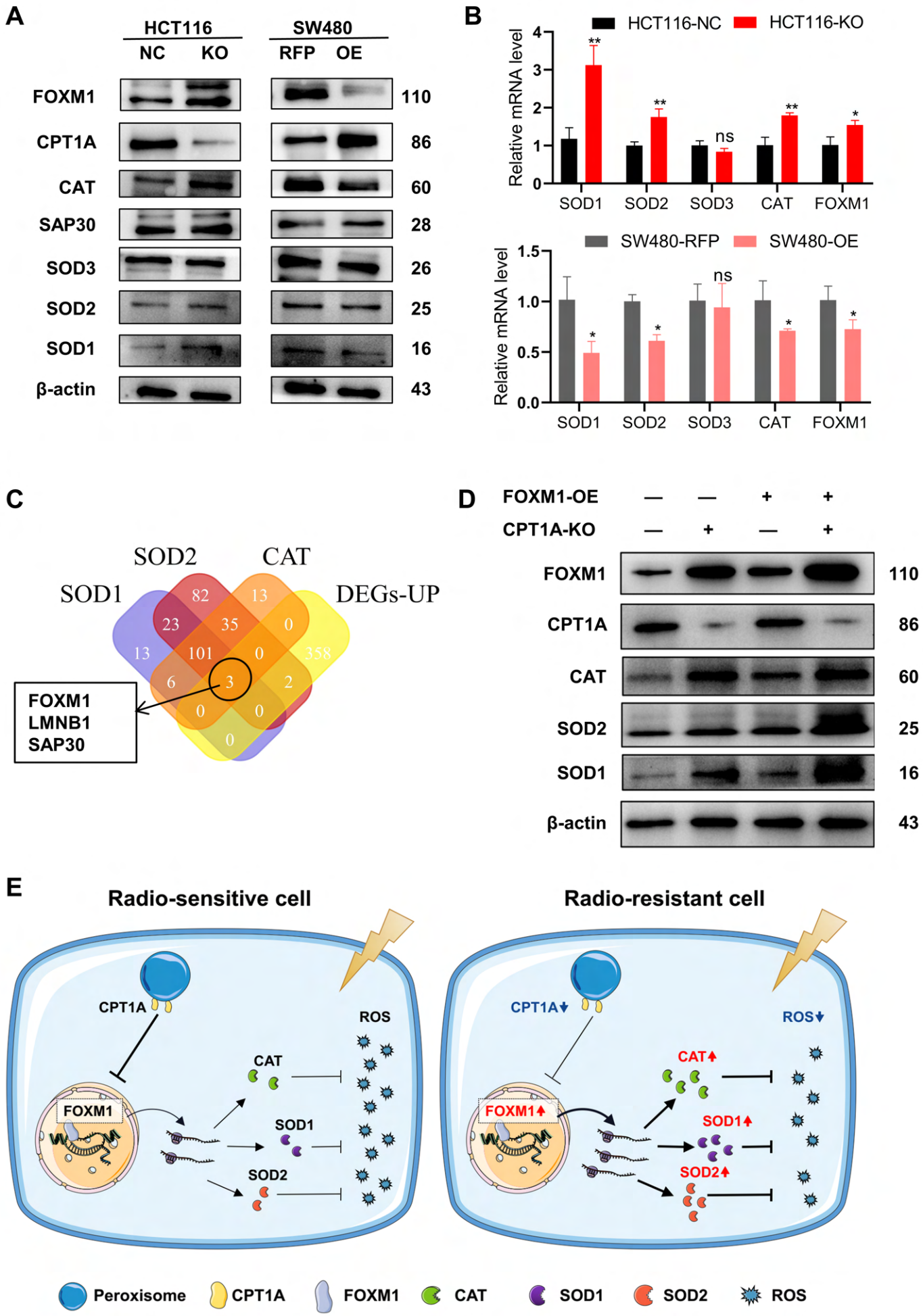
A
HCT116
NC
KO
SW480
RFP
OE
FOXM1
CPT1A
CAT
SAP30
SOD3
SOD2
SOD1
β-actin
110
86
60
28
26
25
16
43
B
HCT116-NC
HCT116-KO
Relative mRNA level
SOD1
SOD2
SOD3
CAT
FOXM1
ns
SW480-RFP
SW480-OE
C
SOD2
CAT
SOD1
DEGs-UP
82
13
23
35
0
13
101
0
358
6
3
2
0
0
0
FOXM1
LMNB1
SAP30
D
FOXM1-OE
CPT1A-KO
E
Radio-sensitive cell
Radio-resistant cell
CPT1A
ROS
CAT
FOXM1
SOD1
SOD2
CPT1A↓
ROS↓
CAT↑
FOXM1↑
SOD1↑
SOD2↑
Peroxisome
CPT1A
FOXM1
CAT
SOD1
SOD2
ROS